ARTICLE

Meteorin-like/Meteorin-β protects heart against cardiac dysfunction

Celia Rupérez[1,2], Gemma Ferrer-Curriu[1,2], Aina Cervera-Barea[1,2], Laura Florit[1,2], Mariona Guitart-Mampel[3,4], Gloria Garrabou[3,4], Mònica Zamora[5], Fàtima Crispi[5], Joaquim Fernandez-Solà[6], Josep Lupón[7], Antoni Bayes-Genis[7], Francesc Villarroya[1,2], and Anna Planavila[1,2]

Meteorin-like/Meteorin-β (Metrnl/Metrnβ) is a secreted protein produced by skeletal muscle and adipose tissue that exerts metabolic actions that improve glucose metabolism. The role of Metrnβ in cardiac disease is completely unknown. Here, we show that *Metrnβ*-null mice exhibit asymmetrical cardiac hypertrophy, fibrosis, and enhanced signs of cardiac dysfunction in response to isoproterenol-induced cardiac hypertrophy and aging. Conversely, adeno-associated virus–mediated specific overexpression of Metrnβ in the heart prevents the development of cardiac remodeling. Furthermore, Metrnβ inhibits cardiac hypertrophy development in cardiomyocytes in vitro, indicating a direct effect on cardiac cells. Antibody-mediated blockage of Metrnβ in cardiomyocyte cell cultures indicated an autocrine action of Metrnβ on the heart, in addition to an endocrine action. Moreover, Metrnβ is highly produced in the heart, and analysis of circulating Metrnβ concentrations in a large cohort of patients reveals that it is a new biomarker of heart failure with an independent prognostic value.

Introduction

Meteorin-β protein (Metrnβ), also known as Meteorin-like (Metrnl) or IL-41 (Ushach et al., 2018; Bridgewood et al., 2019; Rao et al., 2014), is a recently identified hormone that is produced by skeletal muscle and adipose tissue upon stimulation by exercise and cold exposure, respectively. Rao et al. (2014) reported that Metrnβ promotes energy expenditure and favors glucose tolerance through the induction of alternatively activated macrophages at adipose depots and promotion of adipose tissue browning. Further research in Metrnβ transgenic mice revealed that peroxisome proliferator–activated receptor-γ (PPARγ) contributes to the beneficial effects of Metrnβ in adipose tissue (Li et al., 2015). In skeletal muscle, Metrnβ attenuates inflammation and insulin resistance via AMP-activated protein kinase and PPARδ-dependent pathways (Jung et al., 2018). Metrnβ has been associated with innate immunity, acquired immunity, and inflammatory pathways and is strongly induced in alternatively activated macrophages (Ushach et al., 2018; Ushach et al., 2015). Recent studies in humans have shown that Metrnβ levels are decreased in obese and diabetic patients and

negatively correlate with glucose levels and insulin resistance (Lee et al., 2018; Pellitero et al., 2018). Metrnβ levels have been associated with the presence and severity of coronary artery disease in humans (Liu et al., 2019). Finally, very recently, it has been shown that Metrnβ attenuates the cardiotoxicity associated with chemotherapy in cancer treatments (Hu et al., 2020). To date, however, the role of Metrnβ during cardiac disease has not been explored.

The term "cardiokine" has emerged in recent years to name proteins secreted from the heart that have autocrine, paracrine, and/or endocrine functions crucial for the maintenance of cardiac function and other systemic actions (Doroudgar and Glembotski, 2011). Because of their extracellular localization, cardiokines show promise as biomarkers, therapeutic targets, or even therapeutic agents (Planavila et al., 2017).

Cardiac hypertrophy and subsequent progression to heart failure (HF) represent a major cause of morbidity and mortality in industrialized countries. The defining features of cardiac hypertrophy are enhanced protein synthesis, increased cardiomyocyte

[1]Departament de Bioquímica i Biologia Molecular, Institut de Biomedicina, Universitat de Barcelona, Barcelona, Spain; [2]Centro de Investigación Biomédica en Red Fisiopatología de la Obesidad y Nutrición, Barcelona, Spain; [3]Muscle Research and Mitochondrial Function Laboratory, Cellex – August Pi i Sunyer Biomedical Research Institute, Faculty of Medicine and Health Science, University of Barcelona, Internal Medicine Service, Hospital Clínic of Barcelona, Barcelona, Spain; [4]Center for Biomedical Research Network on Rare Diseases, Barcelona, Spain; [5]Fetal I+D Fetal Medicine Research Center, BCNatal - Barcelona Center for Maternal-Fetal and Neonatal Medicine (Hospital Clinic and Hospital San Juan de Deu), Institut Clinic de Ginecologia, Obstetricia i Neonatalogia, August Pi i Sunyer Biomedical Research Institute, University of Barcelona, Barcelona, Spain; [6]Department of Medicine, Hospital Clinic, University of Barcelona, Barcelona, Spain; [7]Heart Institute, Germans Trias i Pujol University Hospital, Center for Biomedical Research Network on Cardiovascular Diseases, Badalona, Spain.

Correspondence to Anna Planavila: aplanavila@ub.edu; Francesc Villarroya: fvillarroya@ub.edu.

size, a greater degree of sarcomere organization, and a shift in the metabolic energy source from fatty acids to glucose (van Bilsen et al., 1998). Inflammation also plays an important role in hypertrophic responses in the heart (Smeets et al., 2008a; Planavila et al., 2011). HF remains a critical health problem, and the identification of underlying molecular targets and novel protective agents is of crucial importance for improving the efficacy of preventive and therapeutic strategies.

The observation of a very high expression of Metrnβ in the heart prompted us to analyze the role of Metrnβ as a secreted protein in cardiac tissue. We observed that mice lacking Metrnβ are prone to develop cardiac alterations and that cardiac-specific recovery of Metrnβ expression prevents hypertrophic induction. Moreover, the signals that promote hypertrophy also induce cardiac Metrnβ expression and protein secretion in vivo and in vitro. Finally, the circulating levels of Metrnβ are increased in HF patients, and Metrnβ appears as a new biomarker for cardiac prognosis in these patients.

Results

Metrnβ is expressed in heart, produced and secreted by cardiomyocytes, and up-regulated upon cardiac stress in mice and humans

We analyzed the relative expression levels of the Metrnβ transcript in various mouse tissues. We found the highest expression level in the heart, where the Metrnβ mRNA level was higher than that found in the other tissues tested, including tissues previously considered to be sources of Metrnβ, such as adipose tissue and skeletal muscle (Fig. 1 a). In human tissue samples, the expression levels of Metrnβ transcript in the heart were lower than in adipose tissue but twice those in liver and skeletal muscle (Fig. S1 a).

Induction of cardiac hypertrophy in distinct experimental models in mice based on treatment with the hypertrophic agent isoproterenol (ISO), transversal aortic constriction (TAC), and angiotensin II (AngII)–induced hypertension significantly increased the expression levels of Metrnβ in mouse heart (Fig. 1 b). Metrnβ circulating levels are significantly induced after ISO-induced cardiac hypertrophy (Fig. 1 c).

Furthermore, Metrnβ transcript expression levels were significantly induced in hearts from human patients suffering from HF (Fig. 1 d). Immunohistochemical analysis revealed a significant increase in the Metrnβ protein levels in patients affected by distinct types of cardiomyopathy (hypertensive, valvular, and idiopathic; Fig. 1 e).

Isolation of cardiac cells from rat heart indicated that Metrnβ is preferentially expressed in cardiomyocytes rather than in cardiac fibroblasts (CFs; Fig. 1 f). Our analysis of Metrnβ expression in primary cultures of neonatal cardiomyocytes (NCMs) showed that Metrnβ mRNA levels were significantly increased following exposure to the hypertrophic agent phenylephrine (PE; Fig. 1 g). Finally, to determine whether Metrnβ was actually secreted by cardiomyocytes, we analyzed Metrnβ protein levels in NCM culture media. The basal rate of Metrnβ secretion in media under control conditions was ∼0.04 ng ml^{-1} 24 h^{-1}. After treatment with PE, the rate of Metrnβ protein secretion by NCMs in culture was significantly increased, reaching ∼0.08 ng ml^{-1} 24 h^{-1} (Fig. 1 g). These results indicate that the heart reacts to hypertrophy induction and other cardiac insults by inducing Metrnβ expression and that cardiomyocytes are active cells for Metrnβ expression and release, especially in response to the induction of cardiac cell hypertrophy.

PPARα controls Metrnβ expression in heart

Next, we analyzed the mechanisms that are responsible for controlling Metrnβ expression and responsiveness in the heart in the context of hypertrophy-inducing conditions. Previous studies showed that the PPARα pathway protects the heart from cardiac hypertrophy (Planavila et al., 2011; Smeets et al., 2008a; Smeets et al., 2007; Smeets et al., 2008b), and members of the PPAR family of transcription factors have been shown to regulate Metrnβ in adipose and skeletal muscle tissues (Jung et al., 2018; Li et al., 2015). Accordingly, we first studied Metrnβ expression in hearts from Pparα-null mice under basal conditions and after ISO treatment–based induction of cardiac hypertrophy (Fig. 1 h). Cardiac Metrnβ expression was reduced in Pparα-null mice under basal conditions. As expected, ISO treatment induced an increase in the Metrnβ mRNA expression levels of WT mice. However, the induction of Metrnβ by ISO was completely abrogated in Pparα-null mice.

The involvement of the PPARα pathway in controlling cardiac Metrnβ expression was further confirmed in vitro in NCMs (Fig. 1 i). Adenoviral vector (Ad)–mediated overexpression of PPARα in NCMs led to a significant increase in both Metrnβ transcript levels and the amount of Metrnβ protein secreted to the culture media. In contrast, the PPARα inhibitor GW6471 significantly attenuated the increase in Metrnβ transcript levels elicited by PE. Collectively, these results indicate that the PPARα pathway critically controls Metrnβ expression in the heart.

Cardiac damage is enhanced in Metrnβ$^{-/-}$ mice

Given our observations that the heart is a relevant expression site and source of Metrnβ, we next analyzed the role of Metrnβ in the heart by determining the impact of Metrnβ ablation (Metrnβ$^{-/-}$) in mice. 2-mo-old Metrnβ$^{-/-}$ mice did not show any marked alteration in general morphometric or metabolic profiles under basal conditions (Table S1). Only reductions in inguinal white adipose tissue depots and reduced triglycerides were observed. No genotype-related difference in blood pressure was found under any tested condition (Table S2). We analyzed the hearts from Metrnβ$^{-/-}$ mice at baseline and after 7 d of exposure to continuous ISO infusion to experimentally induce cardiac hypertrophy. Histological examination of H&E-stained left ventricular posterior wall (LVPW) and septum tissue sections revealed that the cardiomyocyte cross-sectional area (CSA) was larger in Metrnβ$^{-/-}$ mice than in WT mice at both sites (Fig. 2, a and b). ISO treatment significantly increased CSA in both Metrnβ$^{-/-}$ and WT mice, but the post-ISO increase in CSA was much greater in the septum of Metrnβ$^{-/-}$ mice. ISO significantly increased the heart weight/tibia length (HW/TL) ratio and the dimensions of interventricular septal (IVS), LVPW, and left ventricular internal diameter (LVID) in systole, regardless of genotype, in our two-way ANOVA analysis, indicating cardiac
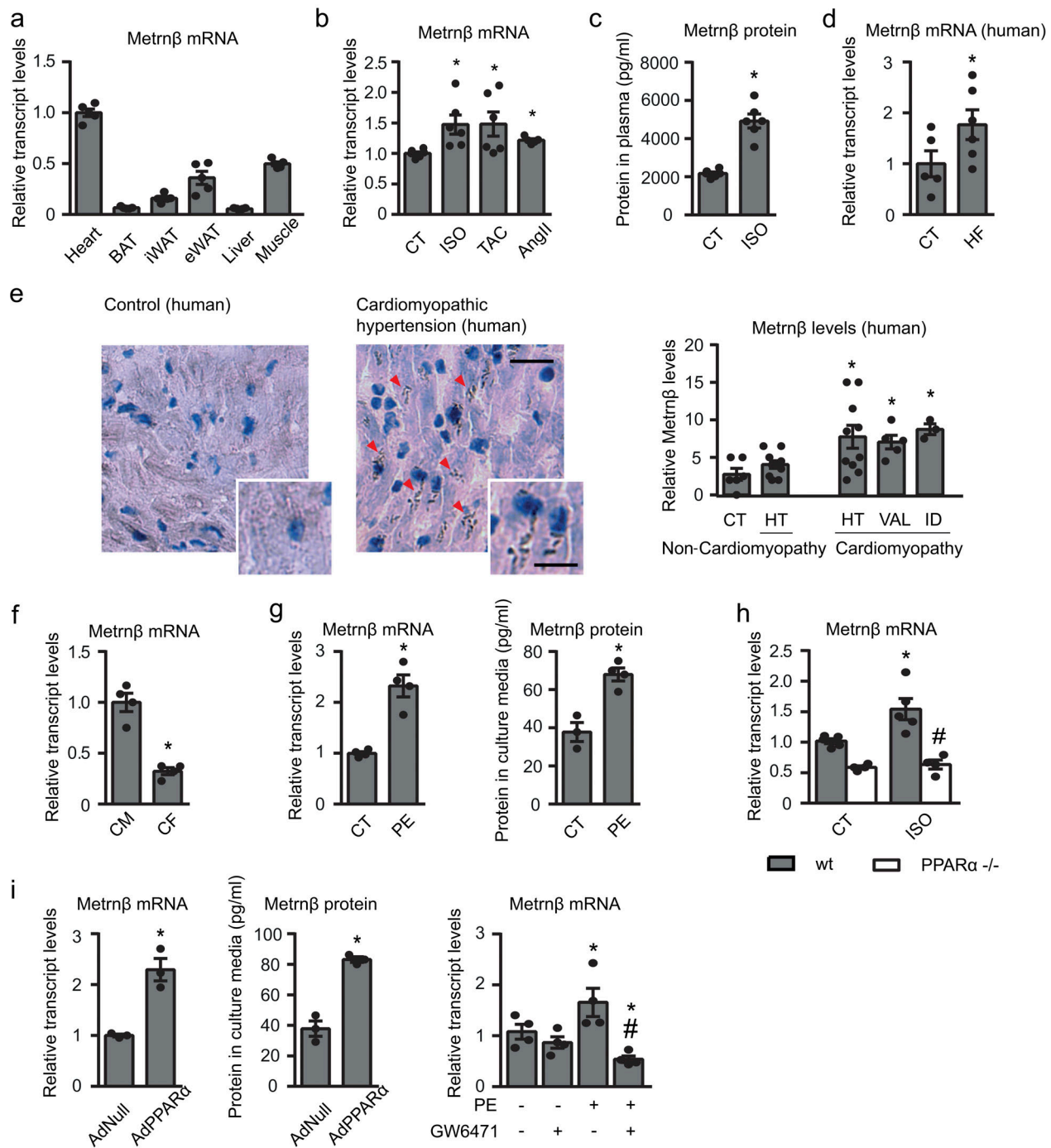
Rupérez et al.
Meteorin-β protects the myocardium

Journal of Experimental Medicine   2 of 18
https://doi.org/10.1084/jem.20201206

Figure 1. Metrnβ is expressed and released by cardiac cells, up-regulated in response to hypertrophic stimuli, and controlled by the PPARα pathway.
(a) Metrnβ expression levels in heart, brown adipose tissue (BAT), inguinal white adipose tissue (iWAT) and epididymal white adipose tissue (eWAT), liver, and skeletal muscle of adult mice (n = 5 mice/group). **(b)** Metrnβ mRNA levels in mouse heart after induction of cardiac hypertrophy by 7 d of ISO infusion, 1 mo of TAC, or 7 d of AngII (n = 6 mice/group; Student's t test; P values are 0.0143, 0.0374, 0.0003). **(c)** Circulating Metrnβ protein levels (n = 6 mice/group; Student's t test; P < 0.0001). **(d)** Cardiac Metrnβ expression levels in control individuals (CT; n = 5) and HF patients (n = 6); Mann-Whitney test; P = 0.0317. **(e)** Metrnβ immunohistochemistry in human hearts and quantification of the Metrnβ expression index as the ratio of positively stained to negatively stained myocytes. CT (n = 6), hypertension (HT; n = 11 non-cardiomyopathy [non-CMP] and n = 10 CMP), valvular (VAL; n = 5), idiopathic (ID; n = 3). Mann-Whitney test; P = 0.0402, 0.0152, 0.0238. Magnification, 20×. Scale bars, 25 μm (inset) and 50 μm. Red arrowheads show positive staining. **(f)** Metrnβ mRNA levels in the CM and CF fractions from isolated rat hearts. Data are representative of four independent experiments; Student's t test; P = 0.0004. **(g)** Metrnβ mRNA levels in NCMs and protein levels in culture media after PE stimulation for 24 h. Data are representative of four independent experiments; Student's t test; P values are 0.0009, 0.0034. **(h)** Metrnβ mRNA levels in WT littermates and PPARα^{−/−} mice injected with ISO (i.p.) for 7 d (n = 5 mice/group; one-way ANOVA; P values are 0.0182, 0.0031). **(i)** Metrnβ mRNA and protein levels in NCMs overexpressing PPARα (AdPPARα) or control vector (AdNull; 10 IFU/cell; data are representative of three independent experiments; Student's t test; P values are 0.0043, 0.001), and Metrnβ mRNA levels in NCMs treated with PE and the PPARα antagonist GW6471 (1 μM), alone or in combination, for 24 h (data are representative of four independent experiments; one-way ANOVA; P values are 0.0494, #0.0077, *0.0448). Results are expressed as mean ± SEM (*, P < 0.05 compared with control human hearts, WT control mice, or control cells; #, P < 0.05 compared with ISO-treated WT animals [h] or PE-stimulated cells [i]).
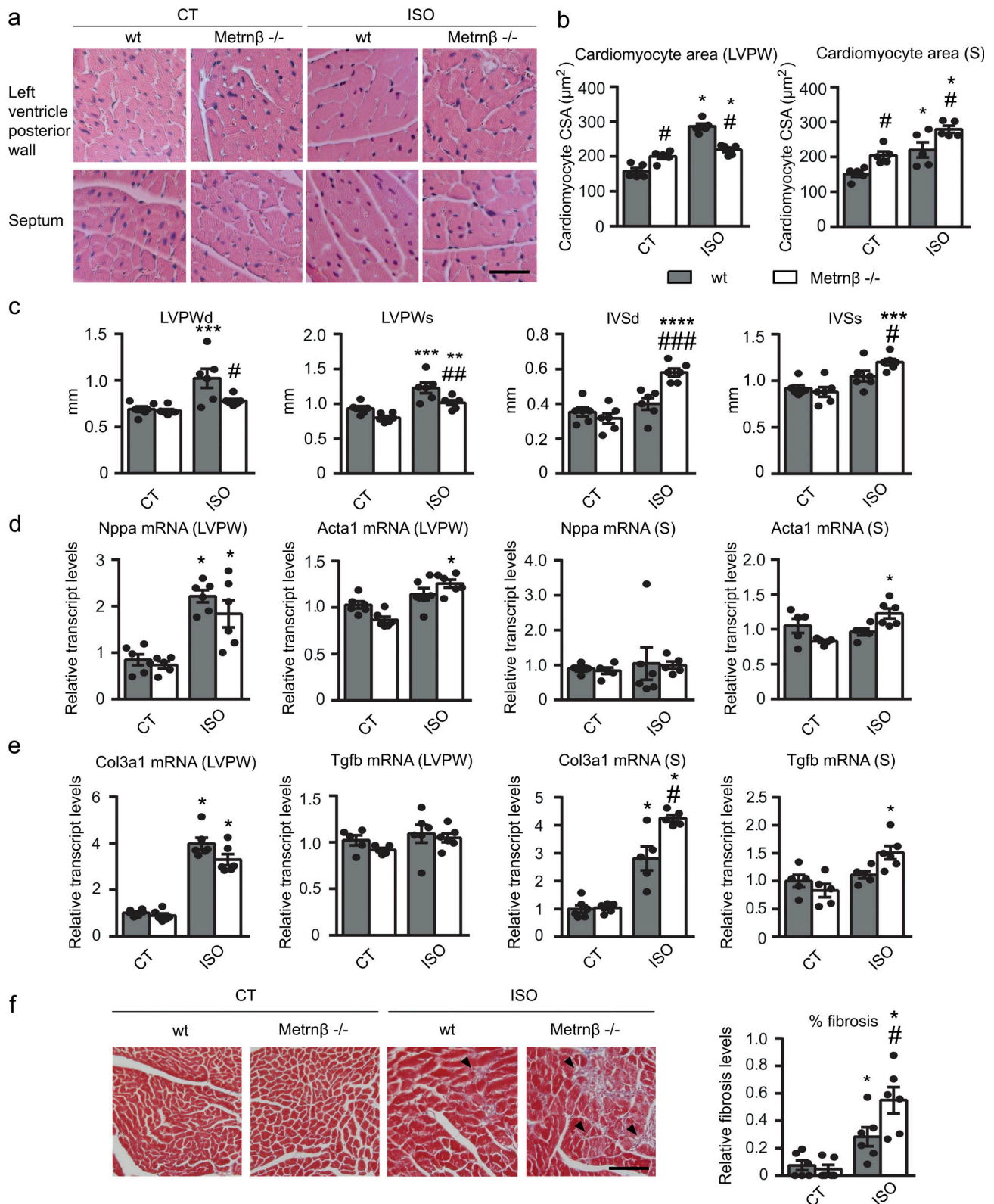
Figure 2. **_Metrnβ_-null mice develop enhanced cardiac alterations in response to ISO infusion.** 2-mo-old WT littermates (gray bars) and _Metrnβ−/−_ (white bars) mice were continuously infused with ISO for 7 d to experimentally induce heart hypertrophy. **(a)** Representative histological sections of hearts stained with H&E were used to determine cardiomyocyte CSA. Magnification, 20×. Scale bar, 50 µm. **(b)** Quantification of cardiomyocyte CSA in the LVPW (P values are 0.0011, <0.0001, 0.0368, <0.0001) and theseptum (S; P values are 0.0008, 0.0047, 0.0001, 0.013). **(c)** IVS and LVPW in systole (s) and diastole (d) assessed by echocardiography. P values are 0.0111, 0.043, 0.0046, 0.0006, 0.0274, <0.0001, 0.0011, 0.0004, 0.0492. **(d)** mRNA expression of the hypertrophy marker genes _Nppa_ and _Acta1_ in the LVPW and the septum (S; P values are <0.0001, 0.0089, <0.0001, 0.0008). **(e)** mRNA expression of the fibrosis markers _Col3a1_ and _Tgfb_ in the LVPW and the septum (S; P values are <0.0001, <0.0001, 0.0018, <0.0001, 0.0122, 0.0031). **(f)** Determination of fibrosis in histological sections by

Masson's trichrome staining. Magnification, 20×. Scale bar, 100 µm. Arrowheads show fibrotic areas (blue; P values are 0.0238, 0.0005, 0.0479). Results are expressed as mean ± SEM; n = 6 mice/group. Data were analyzed by one-way ANOVA (*, P < 0.05; **, P < 0.001; ***, P < 0.0001, ****, P <0.00001 compared with corresponding control [CT] mice; #, P < 0.05; ##, P < 0.001; ###, P < 0.0001 compared with corresponding WT mice).

hypertrophy development (Fig. 2 c and Table 1). However, $Metrn\beta^{-/-}$ mice exhibited exacerbated induction of cardiac IVS after diastole (IVSd) and IVS dimensions in response to ISO, whereas they also showed a lesser increase in LVPWd and LVPW dimensions.

Thus, it was concluded that the absence of Metrnβ caused an abnormal cardiac remodeling, causing a much greater increase in the thickness and area of the cardiomyocytes, especially in the IVS in response to ISO-induced hypertrophic challenge.

The morphological signs of heart alterations in $Metrn\beta^{-/-}$ mice were accompanied by functional disturbances (Table 1). Left ventricular ejection fraction (LVEF) and fractional shortening (FS) were significantly increased by ISO treatment in $Metrn\beta^{-/-}$ mice. Doppler measurements showed a significant increase in the aortic peak velocity, a measure of cardiac contractility, and aortic diameter in response to ISO treatment in both genotypes, although the values were greater in $Metrn\beta^{-/-}$ mice. The parameters of diastolic function E peak and mitral deceleration were altered in $Metrn\beta^{-/-}$ mice: E peak tended to increase in $Metrn\beta^{-/-}$ mice after ISO treatment (P = 0.06), and

mitral deceleration was significantly reduced in mice lacking Metrnβ, indicating reduced relaxation times during diastole. Collectively, these data indicate that the asymmetrical hypertrophy developed in $Metrn\beta^{-/-}$ mice is associated with a higher degree of contractility necessary to compensate the thickening of the septal wall, a phenotype resembling patients with hypertrophic cardiomyopathy (Marian and Braunwald, 2017; Yousefzai et al., 2017).

The mRNA expression levels of the hypertrophy marker genes encoding atrial natriuretic factor (Nppa) and α-actinin (Acta1) were similar in WT and $Metrn\beta^{-/-}$ mice under basal conditions (Fig. 2 d). In the LVPW, ISO infusion caused similar increases in Nppa in both genotypes but triggered a significant induction of Acta1 only in $Metrn\beta^{-/-}$ mice. In the septum, ISO infusion caused no increase in Nppa in both genotypes, but it also triggered a significant induction of Acta1 only in $Metrn\beta^{-/-}$ mice. To assess fibrosis, we performed Masson's trichrome staining and evaluated the expression of collagen 3 (Col3a1) and Tgfb transcripts (Fig. 2, e and f). These measures together showed that ISO triggered fibrosis-related parameters more

Table 1. **Echocardiographic data from 2-mo-old WT and Metrnβ⁻/⁻ mice after ISO-induced hypertrophy**

	CT		ISO		
	WT	**Metrnβ⁻/⁻**	**WT**	**Metrnβ⁻/⁻**	**P value**
HW/TL (mg/mm)	6.88 ± 0.16	7.32 ± 0.38	8.75 ± 0.33***	8.59 ± 0.18**	****
HW/BW (mg/g)	4.10 ± 0.11	4.35 ± 0.12	5.20 ± 0.21***	5.05 ± 0.20*	****
IVSd (mm)	0.57 ± 0.01	0.56 ± 0.01	0.60 ± 0.02	0.69 ± 0.01****,###	****, #, $$$
LVPWd (mm)	0.69 ± 0.03	0.67 ± 0.02	0.94 ± 0.08***	0.78 ± 0.02#	***, #
LVIDd (mm)	4.21 ± 0.08	4.05 ± 0.13	4.14 ± 0.06	4.15 ± 0.04	
IVSs (mm)	0.92 ± 0.03	0.88 ± 0.05	1.05 ± 0.06	1.22 ± 0.03***,#	****, $
LVPWs (mm)	0.93 ± 0.03	0.80 ± 0.02	1.23 ± 0.07***	1.02 ± 0.03**,##	****, ##
LVIDs (mm)	3.08 ± 0.07	3.27 ± 0.04	2.96 ± 0.07	2.97 ± 0.03**	**
EF (%)	59.3 ± 1.1	50.8 ± 2.1##	61.2 ± 1.2	62.3 ± 1.1****	***, #, $$
FS (%)	27.2 ± 0.6	23.0 ± 0.7##	27.8 ± 0.8	28.8 ± 0.7****	***, #, $$
EDV (mm³)	79.4 ± 3.5	77.7 ± 3.7	76.1 ± 2.7	76.28 ± 1.8	
ESV (mm³)	37.5 ± 2.1	43.1 ± 1.2	34.1 ± 2.1	34.2 ± 0.9**	**
Heart rate	308.2 ± 25.9	358.6 ± 28.9	474.6 ± 37.3***	511.8 ± 11.22**	****
LVm (mg)	93.3 ± 2.4	84.2 ± 2.9	126.5 ± 11.3**	110.3 ± 4.0*	**
Aortic peak (m/s)	1.11 ± 0.07	1.24 ± 0.06	1.39 ± 0.09*	1.54 ± 0.07*	**
VTI (cm)	6.43 ± 0.53	6.56 ± 0.29	5.30 ± 0.65	5.70 ± 0.42	
E peak (m/s)	1.09 ± 0.10	0.98 ± 0.10	1.18 ± 0.05	1.26 ± 0.06	
Mitral deceleration (ms)	36.0 ± 2.7	30.2 ± 0.6	31.0 ± 1.8	27.3 ± 1.3	*, #
Aortic diameter (mm)	1.12 ± 0.02	1.20 ± 0.07	1.36 ± 0.01**	1.43 ± 0.07*	***

All measurements are expressed as mean ± SEM; n = 6 mice/group. Data were analyzed by two-way ANOVA, where *, P < 0.05, **, P < 0.001, ***, P < 0.0001, ****, P < 0.00001 for ISO effect; #, P < 0.05, ##, P < 0.001, ###, P < 0.0001 for genotype effect; $, P < 0.05, $$, P < 0.001, $$$, P < 0.0001 for interaction effect. CT, control; d, after diastole; EDV, end diastolic volume; HW/BW, heart weight/body weight ratio; s, after systole.

Table 2. Echocardiographic data from 6- and 16-mo-old WT and Metrnβ−/− mice

	6 mo old		16 mo old		
	WT	**Metrnβ−/−**	**WT**	**Metrnβ−/−**	**P value**
IVSd (mm)	0.57 ± 0.01	0.72 ± 0.03#	0.64 ± 0.01	0.85 ± 0.06##	*, ###
LVPWd (mm)	0.59 ± 0.03	0.71 ± 0.02#	0.68 ± 0.01	0.69 ± 0.02	#
LVIDd (mm)	4.37 ± 0.02	4.30 ± 0.11	4.41 ± 0.06	4.58 ± 0.12	
IVSs (mm)	0.98 ± 0.02	1.12 ± 0.04#	1.06 ± 0.01	1.32 ± 0.04**,###	**, ####
LVPWs (mm)	0.82 ± 0.03	0.91 ± 0.03	0.80 ± 0.02	0.84 ± 0.03	#
LVIDs (mm)	3.21 ± 0.11	3.30 ± 0.15	3.52 ± 0.05	3.60 ± 0.12	*
EF (%)	58.2 ± 3.7	53.8 ± 2.8	47.0 ± 0.4*	49.4 ± 2.1	**
FS (%)	26.5 ± 2.4	23.8 ± 1.7	20.0 ± 0.4*	21.2 ± 1.1	
EDV (mm^3)	86.4 ± 1.2	83.6 ± 5.2	88.5 ± 3.1	96.7 ± 5.7	
ESV (mm^3)	41.76 ± 3.6	44.65 ± 4.7	51.79 ± 1.7	55.0 ± 4.4	*
Heart rate	337.3 ± 17.4	352.6 ± 17.2	381.3 ± 18.6	382.6 ± 12.0	*
LVm (mg)	89.9 ± 2.2	113.4 ± 6.4#	107.1 ± 1.8	148.1 ± 8.6**,###	***, ####
Aortic peak (m/s)	1.02 ± 0.06	0.90 ± 0.03	0.84 ± 0.04	1.07 ± 0.05*##	$$
VTI (cm)	5.72 ± 0.52	5.00 ± 0.19	4.60 ± 0.23	5.14 ± 0.23	
E peak (m/s)	0.78 ± 0.06	0.91 ± 0.06	0.83 ± 0.01	0.98 ± 0.05	#
Mitral deceleration (ms)	26.7 ± 2.1	27.4 ± 1.6	23.7 ± 1.3	26.6 ± 1.7	
Aortic diameter (mm)	1.15 ± 0.01	1.23 ± 0.03	1.24 ± 0.01	1.32 ± 0.05	*, #

All measurements are expressed as mean ± SEM; n = 5 mice/group. Data were analyzed by two-way ANOVA, where *, P < 0.05, **, P < 0.001, ***, P < 0.0001 for 16-mo-old effect; #, P < 0.05, ##, P < 0.001, ###, P < 0.0001, ####, P < 0.00001 for genotype effect; $$, P < 0.001 for interaction effect. d, after diastole; EDV, end diastolic volume; s, after systole.

intensely in *Metrnβ−/−* mice than in WT mice in the septum, but not in the LVPW. Moreover, we analyzed the expression levels of negative regulators of apoptosis, such as *Bcl-2*, *Bcl-xl*, and *XIAP*, in these animals (Fig. S2 a). At basal levels, we did not observe significant differences due to genotype. After ISO treatment, we found a significant increase in all genes—*Bcl-2*, *Bcl-xl*, and *XIAP*—similar in both genotypes. These data suggest an inhibition of the apoptotic processes due to ISO, regardless of genotype.

Collectively, our findings indicate that the lack of Metrnβ alters the heart, mostly promoting asymmetrical cardiac hypertrophy characterized by left ventricular dysfunction and enhancing interstitial fibrosis.

Finally, in order to confirm the role of Metrnβ favoring asymmetrical cardiac hypertrophy, observed above in mice lacking Metrnβ under the ISO induction model, we analyzed the effects of Metrnβ invalidation in the aging-associated cardiac remodeling process. For this purpose, we performed echocardiography assessments of *Metrnβ−/−* and WT mice at two distinct ages: 6 and 16 mo old (Table 2). We found that aging led to a significant increase in LVPWd, IVS, LVID, end systolic volume (ESV), and left ventricular mass (LVm) in both genotypes. However, the increase in IVS, LVPW, and LVm was significantly higher in *Metrnβ−/−* mice compared with WT mice. Regarding systolic function, we found a similar decrease in ejection fraction (EF) over time in both genotypes. Aging led to a significant increase in aortic diameter in both genotypes. However, aortic

diameter, aortic peak, and E peak were significantly increased in 16-mo-old *Metrnβ−/−* mice compared with their corresponding age-matched WT mice; such a difference was already statistically significant for aortic diameter and E peak at the 6-mo-old aging stage.

Collectively, these data confirmed the susceptibility of *Metrnβ−/−* mice to spontaneously develop cardiac interventricular hypertrophy and systolic and diastolic dysfunction in aging.

Cardiac-specific overexpression of Metrnβ prevents cardiac hypertrophy development

To further investigate the function of Metrnβ in cardiac biology, we set out to increase mouse Metrnβ expression specifically in the heart. AAV9 is known to preferentially target the heart, and specifically the cardiomyocytes, with minimal transduction of other tissues and cell types (Bär et al., 2014). We found that, under our experimental conditions of delivery in vivo, immunohistochemical detection of enhanced GFP (eGFP) showed that an AAV9 reporter vector (AAV9-CMV-eGFP) transduced higher in heart cells than in cells in WAT, liver, or muscle (Fig. S1 b). Specific AAV9-mediated expression of Metrnβ in the heart was confirmed by our observations that *Metrnβ−/−* mice injected with AAV9-Metrnβ exhibited high Metrnβ transcript expression in the heart, much lower expression in the skeletal muscle, and almost no expression in the other analyzed tissues (Fig. S1 c). We found that AAV-mediated targeting of Metrnβ expression in the heart normalized (and even increased) circulating Metrnβ levels

in *Metrnβ−/−* mice (Fig. S1 d), which supports the notion that heart-originating Metrnβ can affect circulating systemic levels.

Since Metrnβ is expressed in many tissues in the body, to elucidate the role of cardiac-originated Metrnβ, we overexpressed Metrnβ in the myocardium of *Metrnβ−/−* mice. *Metrnβ−/−* mice were injected with AAV9 vectors preferentially targeting cardiomyocytes, AAV9-null (used as control vector) or AAV9-Metrnβ and were continuously infused with ISO for 7 d to induce cardiac hypertrophy (Fig. 3). As expected, after 7 d of ISO infusion, the HW/TL ratio was significantly increased in AAV9-null–injected *Metrnβ−/−* mice compared with non–ISO-treated *Metrnβ−/−* mice. In contrast, the HW/TL ratio (indicative of the development of cardiac hypertrophy) was significantly reduced in *Metrnβ−/−* mice in which Metrnβ expression in the heart has been induced by AAV9-Metrnβ injection (Fig. 3 a). No difference in blood pressure was found under the conditions tested (Table S2). Histological examination of H&E-stained LVPW and septum tissue sections confirmed that the CSA was significantly smaller in ISO-treated *Metrnβ−/−* mice injected with AAV9-Metrnβ than in corresponding ISO-treated *Metrnβ−/−* mice injected with AAV9-null vector (Fig. 3, b and c). The effects were especially marked in the septum, where CSA increase due to ISO was fully prevented by AAV9-Metrnβ–mediated delivery.

Echocardiographic parameters (Table 3) revealed that ISO increased IVS, LVPW, and LVm in both conditions, as expected. However, the LVm calculated by echocardiography and IVS was significantly reduced in ISO-treated AAV9-Metrnβ–injected mice compared with the corresponding AAV9-null–injected mice, indicating that the former mice had undergone reversion of cardiac hypertrophy. EF and FS were similarly increased after ISO treatment in both conditions, but the aortic peak and velocity time integral (VTI) were significantly decreased in AAV9-Metrnβ–injected mice.

The expression of the cardiac hypertrophy marker genes *Nppa* and *Acta1* was similar in *Metrnβ−/−* mice, irrespective of injection with AAV9-Metrnβ or the AAV9-null control vector (Fig. 3 d). However, ISO infusion increased the mRNA expression levels of *Nppa* and *Acta1* in AAV9-null–injected mice, but this effect was significantly blunted in ISO-treated AAV9-Metrnβ–injected mice. We also found that ISO led to a substantial increase in fibrosis (as assessed by Masson's trichrome staining) and concomitant expression of *Col3a1* and *Tgfb* in AAV9-null–injected *Metrnβ−/−* mice, but not in AAV9-Metrnβ–injected mice (Fig. 3, e and f).

Based on these findings, we conclude that cardiac overexpression of Metrnβ prevents cardiac hypertrophy and fibrosis in *Metrnβ−/−* mice in an autocrine manner.

Next, we performed the same experiment in WT mice injected with AAV9-null or AAV9-Metrnβ and infused with ISO for 7 d to induce cardiac hypertrophy (Fig. 3 g). HW/TL ratio was significantly increased by ISO in both AAV9-null– and AAV9-Metrnβ–injected mice compared with their corresponding controls. However, HW/TL ratio was significantly reduced in AAV9-Metrnβ–injected WT mice compared with their corresponding AAV9-null–injected mice subjected to ISO. Echocardiographic measurements showed a significant increase in LVm, IVSd, LVPWd, and aortic peak in AAV9-null–injected mice

subjected to ISO but not in AAV9-Metrnβ–injected mice. The mRNA expression levels of *Nppa* were significantly induced by ISO in AAV9-null–injected mice and significantly reduced in AAV9-Metrnβ–injected mice. Finally, ISO led to an increased expression of *Col3a1* in AAV9-null–injected WT mice and in AAV9-Metrnβ–injected mice. However, *Col3a1* mRNA levels were significantly lower in AAV9-Metrnβ–injected mice. These data indicate that cardiac overexpression of Metrnβ also prevents cardiac hypertrophy and fibrosis development in WT mice.

Metrnβ induces the gene programs of fatty acid oxidation (FAO) and alternatively activated (M2) macrophages in cardiac tissue in vivo

Given that there is a close association between impaired FAO and cardiac hypertrophy (Smeets et al., 2008a; Planavila et al., 2005b), we examined the expression of FAO-related genes. The transcript levels of pyruvate dehydrogenase kinase-4 (*Pdk4*), carnitine palmitoyltransferase (*Cpt1b*), medium-chain acyl-CoA dehydrogenase (*Acadm*), and PPARγ coactivator-1α (PGC1-α, *Ppargc1a*) were markedly decreased in AAV9-null–injected *Metrnβ−/−* mice after ISO treatment, as expected (Fig. 4 a). AAV9-Metrnβ vector–mediated overexpression of Metrnβ in the heart led to a significant up-regulation of *Pdk4* and *Ppargc1a* transcript levels in the heart. Moreover, the protein levels of PGC1-α were significantly increased in cardiac tissue of mice overexpressing Metrnβ (Fig. 4 b).

Overall, these findings indicate that overexpression of Metrnβ and subsequent cardiac hypertrophy reversion are associated with activation of the PGC1-α and FAO pathways.

Given these findings, we analyzed the expression levels of FAO-related genes in the *Metrnβ−/−* mice compared with WT mice (Fig. 4). We found that the expression levels of FAO-related genes were greatly reduced in *Metrnβ−/−* mice under both basal and ISO-exposed conditions compared with WT mice (Fig. 4 c).

Considering that a proinflammatory status is often associated with cardiac hypertrophy development, and considering that it has been reported that Metrnβ modulates systemic and adipose tissue inflammatory pathways in different ways (Rao et al., 2014; Ushach et al., 2018), we next assessed the expression levels of genes involved in proinflammatory type 1 cytokine signaling, such as *Il6*, MCP-1 (*Ccl2*), and TNFα (*Tnfa*), in the hearts of Metrnβ-overexpressing mice (Fig. 4 d). We found that ISO induced *Il6*, *Ccl2*, and *Tnfα* in AAV9-null–injected *Metrnβ−/−* hearts but not in AAV9-Metrnβ–injected *Metrnβ−/−* hearts, in which the expression levels of *Ccl2* and *Tnfα* were significantly reduced. Next, we analyzed the mRNA levels of anti-inflammatory genes associated with type 2 cytokine signaling, such as *Arg1*, *Cd163*, and *Mrc1* (Fig. 4 e). We found that cardiac Metrnβ overexpression up-regulated the transcript levels of these genes and, more important, that the ratio M1/M2 macrophages estimated on the basis of the *iNOS/Arg1* ratio (Redondo-Angulo et al., 2016; Cereijo et al., 2018) was significantly down-regulated in the hearts of Metrnβ-overexpressing mice (Fig. 4 f). Finally, immunostaining of total macrophages (F4/F80-positive cells) in these hearts indicated that there was no difference in the total macrophage population under any of the tested conditions
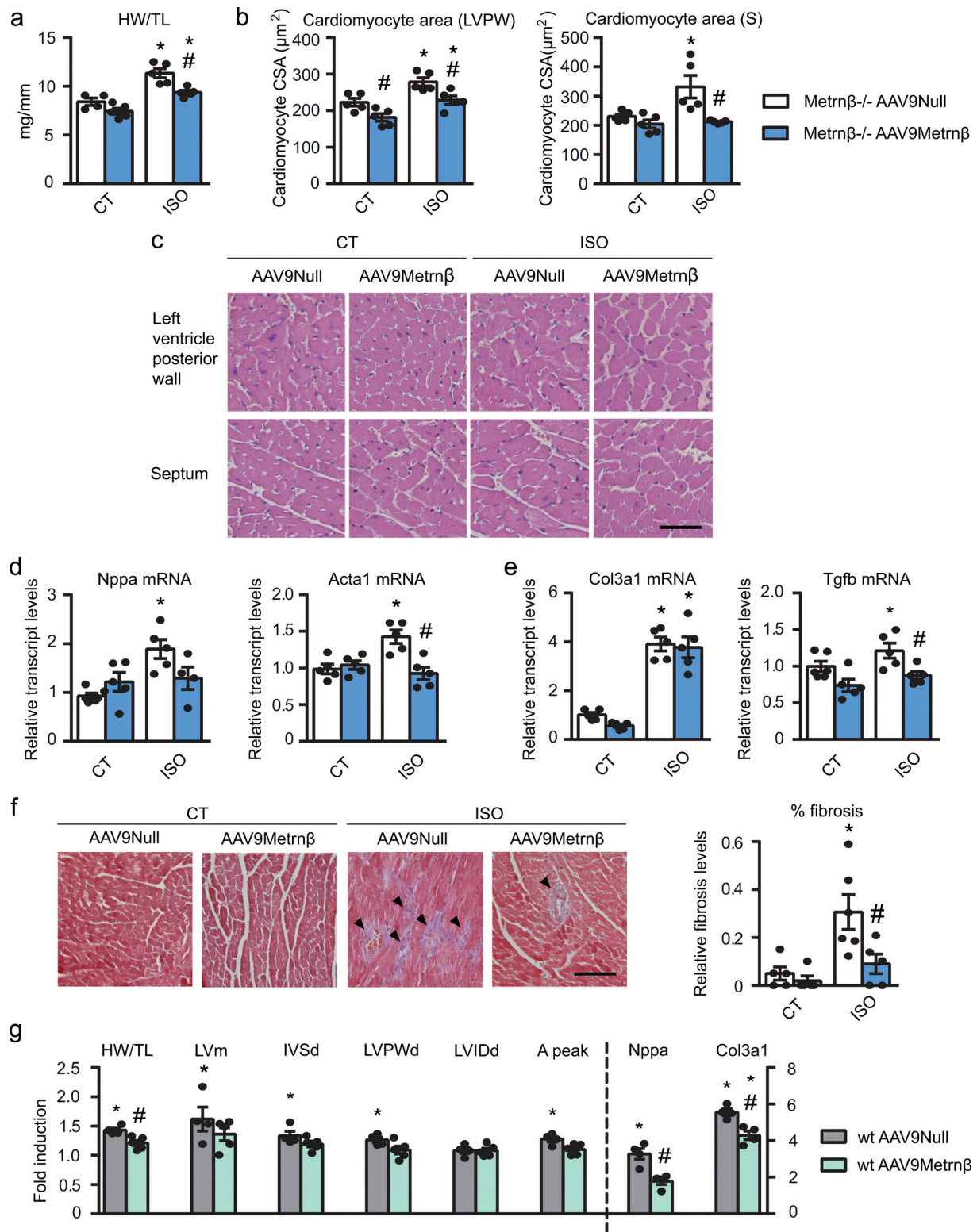
Figure 3. **Metrnβ prevents the development of cardiac hypertrophy in vivo. (a–f)** 2-mo-old *Metrnβ*⁻/⁻ mice were injected i.p. with AAV9 carrying Metrnβ (AAV9-Metrnβ; blue bars) or AAV9-null (white bars) and were continuously infused with ISO for 7 d to induce cardiac hypertrophy. **(a)** HW/TL ratio (P values are 0.0023, 0.001, 0.0053). **(b)** Quantification of cardiomyocyte CSA in the LVPW and the septum (S; P values are 0.0225, 0.0067, 0.0148, 0.0138, 0.0328, 0.0143). **(c)** Representative histological sections of hearts stained with H&E, which were used to determine cardiomyocyte CSA. Magnification, 20×. Scale bar, 50 μm. **(d)** mRNA expression of the hypertrophy markers *Nppa* and *Acta1* in the heart (P = 0.0006). **(e)** mRNA expression levels of the fibrosis markers *Col3a1* and *Tgfb* (P values are <0.0001, <0.0001, 0.0312, 0.0198). **(f)** Determination of fibrosis in histological sections by Masson's trichrome staining. Magnification, 20×. Scale bar, 100 μm. Arrowheads show fibrotic areas (blue; P values are 0.0137, 0.0365, 0.0088). **(g)** 2-mo-old WT mice were injected i.p. with AAV9 carrying Metrnβ (AAV9-Metrnβ; green bars) or AAV9-null (gray bars) and were continuously infused with ISO for 7 d to induce cardiac hypertrophy. HW/TL

ratio, LVm, IVS dimension, LVPW, and LVID after diastole (IVSd, LVPWd, and LVIDd, respectively), aortic (A) peak, and mRNA expression levels of *Nppa* and *Col3a1*. Values are expressed as fold induction (ISO mice versus their corresponding control mice). (P values are 0.0294, 0.032, 0.0032, 0.0215, 0.0088, 0.0265, 0.0002, <0.0001, 0.0011). *n* = 5 mice/group. Results are expressed as mean ± SEM; data were analyzed by one-way ANOVA (*, P < 0.05 compared with corresponding control [CT] mice; #, P < 0.05 compared with corresponding AAV9-null mice).

([Fig. 4 g](#)). Since eosinophils have been reported as targets of Metrnβ in adipose tissue ([Rao et al., 2014](#)), we next studied the expression of the genes encoding Il4 and Il13, which are produced by eosinophils, among other cell types, in the hearts of these mice; however, we were unable to detect any significant expression of *Il4* or *Il13* under any of the tested conditions. Altogether, these data indicate that Metrnβ does not generate a massive change in the total amount of macrophages in the heart, but rather induces a shift toward a noninflammatory environment in the myocardium.

Finally, we analyzed the inflammatory genes in the model of *Metrnβ^{−/−}* mice. We found that although the proinflammatory genes *Il6*, *MCP-1* (*Ccl2*), and *TNFα* (*Tnfa*) were up-regulated upon ISO treatment regardless of genotype ([Fig. 4 h](#)), the genes encoding anti-inflammatory type 2 cytokine signaling components were up-regulated in WT mice but not in *Metrnβ^{−/−}* mice after hypertrophy induction ([Fig. 4 i](#)).

Metrnβ directly targets cardiac cells and prevents cardiomyocyte hypertrophy

To establish whether the effects of Metrnβ observed in our in vivo studies involve a direct action of Metrnβ on cardiomyocytes, we used primary cultured NCMs for experiments in vitro. We investigated the effects of Metrnβ using the standard PE treatment model to induce cardiac cell hypertrophy. PE treatment increased CSA (an indication of cell hypertrophy), whereas Metrnβ significantly attenuated this PE-induced cell enlargement ([Fig. 5, a and b](#)). The transcript levels of the molecular markers of hypertrophy, *Nppa* and *Acta1*, were increased in association with PE-induced hypertrophy, and this effect was reduced by treatment with Metrnβ. Moreover, overexpression of Metrnβ via Ad-mediated transduction prevented the PE-induced hypertrophy of these cells ([Fig. 5, c and d](#)). Furthermore, we found that in PE-induced hypertrophy in which NCMs were additionally treated with proinflammatory factors (TNFα or LPS), overexpression of Metrnβ retained its capacity to prevent hypertrophy development ([Fig. S2 b](#)).

As reported previously ([Ferrer-Curriu et al., 2019](#); [Teunissen et al., 2007](#)), rat CFs cultured on a rigid substrate show progressive fibroblast-to-myofibroblast differentiation, such that passage 1 (P1) cells are considered CFs and P3 cells are considered cardiac myofibroblasts (CMFs) based on the marked increase in α-smooth muscle actin (α-SMA, *Acta2*). We confirmed that the mRNA and protein levels of α-SMA (Acta2) were

Table 3. Echocardiographic data from Metrnβ^{−/−} mice injected with AAV9-Metrnβ or AAV9-null after ISO-induced hypertrophy

	CT		ISO		
	AAV-null	AAV-Metrnβ	AAV-null	AAV-Metrnβ	P value
IVSd (mm)	0.59 ± 0.3	0.53 ± 0.3	0.87 ± 0.04***	0.76 ± 0.04**	****, #
LVPWd (mm)	0.64 ± 0.02	0.66 ± 0.04	0.85 ± 0.04**	0.80 ± 0.04	***
LVIDd (mm)	4.34 ± 0.3	4.26 ± 0.16	4.55 ± 0.08	4.30 ± 0.13	
IVSs (mm)	1.02 ± 0.04	0.80 ± 0.06#	1.48 ± 0.07****	1.25 ± 0.02***,#	****, ###
LVPWs (mm)	0.76 ± 0.02	0.84 ± 0.05	1.11 ± 0.05***	1.15 ± 0.09**	****
LVIDs (mm)	3.23 ± 0.27	3.41 ± 0.17	3.24 ± 0.13	3.15 ± 0.19	
EF (%)	57.4 ± 2.7	47.2 ± 3.3	61.7 ± 3.3	59.0 ± 4.1	*
FS (%)	26.0 ± 1.7	20.4 ± 1.7	28.8 ± 2.1	27.0 ± 2.5	*
EDV (mm³)	87.5 ± 13.8	81.9 ± 7.2	95.1 ± 4.3	83.4 ± 6.1	
ESV (mm³)	43.9 ± 9.0	48.4 ± 5.8	42.8 ± 4.2	40.2 ± 5.5	
Heart rate	392.6 ± 27.1	292.6 ± 28.1##	485.2 ± 8.8**	453.4 ± 12.9****	****, ##
LVm (mg)	108.6 ± 10.1	88.2 ± 5.3	164.3 ± 2.9**	123.8 ± 16.3*,#	***, ##
Aortic peak (m/s)	1.08 ± 0.04	0.76 ± 0.07##	1.21 ± 0.06	0.89 ± 0.05##	*, ####
VTI (cm)	4.66 ± 0.27	4.08 ± 0.55	4.93 ± 0.44	3.60 ± 0.42	#
E peak (m/s)	0.78 ± 0.04	0.68 ± 0.05	0.88 ± 0.09	0.86 ± 0.07	
Mitral deceleration (ms)	27.0 ± 3.1	27.4 ± 1.5	25.2 ± 1.5	29.5 ± 1.9	

All measurements are expressed as mean ± SEM; *n* = 5 mice/group. Data were analyzed by two-way ANOVA, where *, P < 0.05, **, P < 0.001, ***, P < 0.0001, ****, P < 0.00001 for ISO effect; #, P < 0.05, ##, P < 0.001, ###, P < 0.0001, ####, P < 0.00001 for AAV9-Metrnβ effect. d, after diastole; EDV, end diastolic volume; s, after systole.
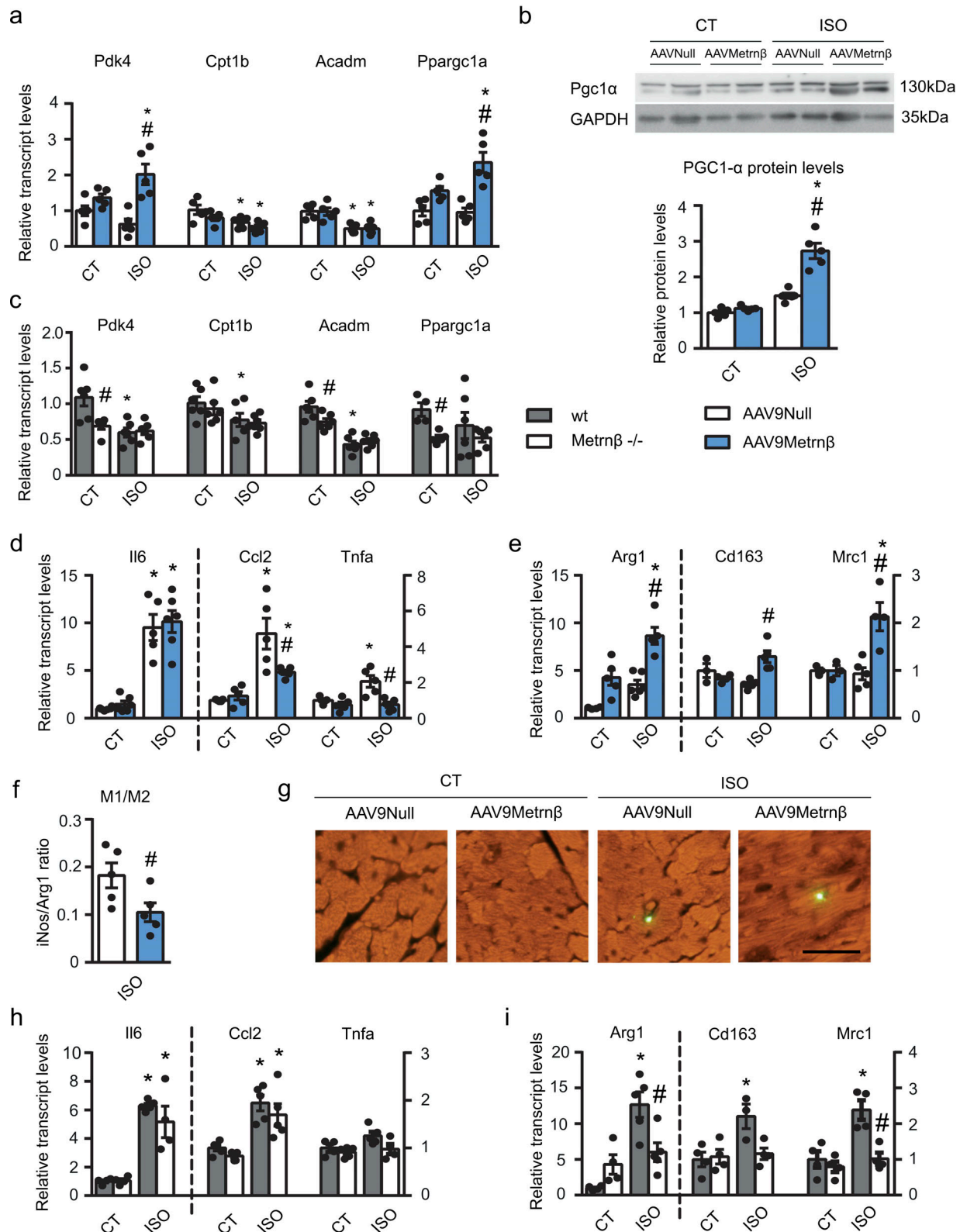
Figure 4. **Fatty acid metabolism, inflammatory signals in heart, and the effects of Metrnβ.** 2-mo-old *Metrnβ*^{−/−} mice were injected i.p. with AAV9 carrying Metrnβ (AAV9-Metrnβ; blue bars) or AAV9-null (white bars; a, b, d–g; *n* = 5 mice/group), or WT littermates (gray bars) and *Metrnβ*^{−/−} (white bars) mice (c, h, i; *n* = 6 mice/group) were continuously infused with ISO for 7 d. **(a)** mRNA expression levels of the lipid catabolism genes *Pdk4*, *Cpt1b*, *Acadm*, and *Ppargc1a* (P values are 0.001, 0.0437, 0.0475, 0.0321, 0.0018, 0.0029, 0.0327, 0.0019). **(b)** PGC1α protein levels in cardiac tissue (P values are <0.0001, 0.0005). **(c)** mRNA expression levels of *Pdk4*, *Cpt1b*, *Acadm*, and *Ppargc1a* (P values are 0.01, 0.0044, 0.0363, 0.0385, 0.0009, 0.0037). **(d)** mRNA expression levels of the proinflammatory genes *Il6*, *Ccl2*, and *Tnfa* (P values are <0.0001, <0.0001, 0.0026, 0.0011, 0.0393, 0.0136, 0.0069). **(e)** mRNA expression levels of the anti-

inflammatory genes *Arg1*, *Cd163*, and *Mrc1* (P values are 0.0064, 0.0004, 0.0023, 0.0263, 0.0051). **(f)** M1/M2 macrophage ratio, which was defined as the *iNos/Arg1* expression level ratio (Student's *t* test; P = 0.0452). **(g)** Macrophages stained with an anti-F4/80 antibody in the heart, assessed by immunofluorescence. Magnification, 20×. Scale bar, 50 μm. **(h)** mRNA expression levels of the proinflammatory genes *Il6*, *Ccl2*, and *Tnfa* (P values are <0.001, 0.0098, 0.0007, 0.0069). **(i)** mRNA expression levels of the anti-inflammatory genes *Arg1*, *Cd163*, and *Mrc1* (P values are 0.0007, 0.0167, 0.0244, 0.0083, 0.0054). Results are expressed as mean ± SEM; data were analyzed by one-way ANOVA (*, P < 0.05 compared with corresponding control [CT] mice; #, P < 0.05 compared with corresponding AAV9-null [a, b, d-g] mice or WT mice [c, h, i]).

increased in P3 cells compared with P1 cells (Fig. 5 e). Treatment of CFs and CMFs with Metrnβ did not modify the mRNA expression and protein levels of α-SMA in CFs or CMFs, indicating that Metrnβ does not have any direct, cell-autonomous effect on cardiac fibrosis in this in vitro model.

Collectively, these data indicate that Metrnβ has direct effects on cardiomyocytes and protects against cardiac hypertrophy and inflammation but does not directly target CFs.

Metrnβ as a cardiokine: Autocrine actions of Metrnβ on cardiac cells

Considering the duality of cardiac cells as both a target and a source of Metrnβ, we examined whether this factor could play an autocrine role (Fig. 5, f and g) by incubating NCMs with an anti-Metrnβ neutralizing antibody. The addition of an Metrnβ-neutralizing antibody to the NCM culture medium significantly increased the CSA of cardiomyocytes and the expression levels of the hypertrophy marker genes *Nppa* and *Acta1*. During the PE-induced enhancement of cardiac hypertrophy, we observed a non-significant tendency for further enhancement of *Nppa* mRNA expression. Taken together, these findings indicate that blocking the activity of endogenously released Metrnβ favors an enhanced hypertrophic state in cardiac cells, thereby confirming an autocrine role for cardiomyocyte-secreted Metrnβ.

Finally, although there is no current knowledge on the identity of cellular receptor(s) for Metrnβ, we explored the intracellular molecular pathway by which Metrnβ may act on cardiac cells. We determined the effects of Metrnβ on a set of putative intracellular kinase-mediated signaling pathways using a multiplex system (Fig. 5 h and Fig. S1 e). We found two proteins involved in intracellular signaling whose phosphorylation status was induced in response to Metrnβ in NCMs: p38-MAPK and the transcription factor CREB (cAMP response element binding). We confirmed phosphorylation of both proteins, p38-MAPK and CREB, in response to Metrnβ in NCMs by Western blot analysis (Fig. 5 h). We also found that the expression of the gene encoding PGC1α, which is a known target of both p38-MAPK and CREB phosphorylation in other cell systems (Villarroya et al., 2018), was induced in response to Metrnβ treatment in cultured cardiomyocytes (Fig. 5 i). Collectively, these findings indicate that, in cardiac cells, Metrnβ directly activates the p38-MAPK and CREB intracellular pathways, which are upstream of the transcriptional regulation of PGC1α.

Metrnβ is a new prognostic biomarker for human HF

Finally, considering that Metrnβ is a secreted protein and that altered levels of cardiokines have been previously proposed as biomarkers of cardiac damage (Bayes-Genis et al., 2012; Bayés-Genís et al., 2015; Lupón et al., 2013), we next explored the value of Metrnβ as a new potential prognostic biomarker in HF. First, we determined the plasma levels of Metrnβ in patients over age (<60 yr old, mean age 45 ± 1.35 [26–60], n = 33; >60 yr old, mean age 80 ± 1.48 [70–96], n = 23; Fig. 6 a). We found that aging led to a significant reduction in Metrnβ circulating levels. Next, we determined Metrnβ circulating levels in control (n = 56; mean age 60 ± 2.63) and HF patients (n = 49; mean age 67 ± 1.7). We found that Metrnβ circulating levels were significantly increased in patients suffering from HF compared with controls (Fig. 6 b). Finally, we examined the predictive value of circulating Metrnβ in a large cohort of 446 patients with HF (mean age, 66.7 yr [59–76], 72.4% male, and median LVEF of 34.8%) to assess mortality risk (Table S3). In a comprehensive multivariable analysis (Table 4) that included Metrnβ, age, sex, LVEF, ischemic etiology, and the presence of diabetes and hypertension, only Metrnβ (hazard ratio [HR], 1.175; 95% confidence interval [CI], 1.009–1.369; P = 0.038), age (HR, 1.055; 95% CI, 1.039–1.071; P < 0.001), and sex (HR, 0.690; 95% CI, 0.483–0.985; P = 0.041) were found to be independent predictors of all-cause death. Interestingly, only age (HR, 1.05; 95% CI, 1.03–1.07; P < 0.001), Metrnβ (HR, 1.12; 95% CI, 1.08–1.71; P = 0.008), and ischemic etiology (HR, 1.70; 95% CI, 1.10–2.65; P = 0.018) were found to be independent predictors of cardiovascular death. In the sensitivity analysis, Metrnβ expressed as quartiles retained independent prognostic value (Table 4). Harrell's C-statistics for the multivariable model including Metrnβ were 0.71 (95% CI, 0.67–0.75) and 0.73 (95% CI, 0.68–0.78) for all-cause and cardiovascular death, respectively. These data indicate that Metrnβ is a promising, powerful new prognostic biomarker for HF.

Discussion

In the present study, we identify Metrnβ as a novel cardiokine, as summarized in Fig. 6 c. We show that the heart is a source of expression and release of Metrnβ as well as a target of Metrnβ. Moreover, we found that Metrnβ exerts a cardioprotective action. Thus, the absence of Metrnβ is associated with cardiac alterations, including asymmetrical hypertrophy, fibrosis, and cardiac dysfunction. Reciprocally, cardiac-specific overexpression of Metrnβ prevents the development of cardiac hypertrophy and fibrosis and restores the normal functioning of the myocardium. Metrnβ can act directly in cardiac cells to protect against hypertrophic processes in mice. In humans, who also express high levels of Metrnβ in the heart, Metrnβ appears to be a strong biomarker of HF prognosis. Overall, our study is the first to show that Metrnβ in the myocardium plays a key role in cardiac pathophysiology.

Our data show that the absence of Metrnβ causes development of an abnormal pattern of asymmetric hypertrophy, with
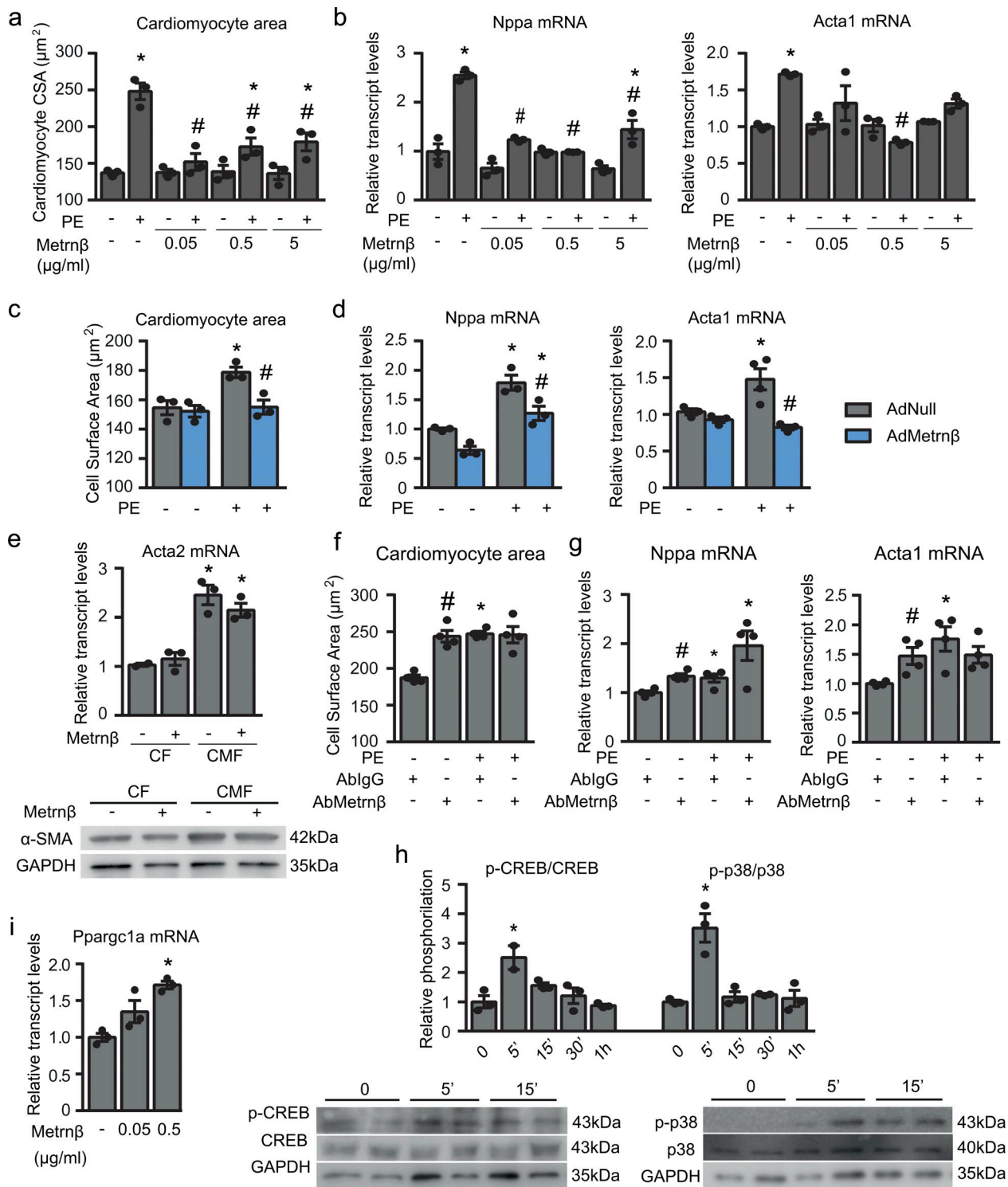
Figure 5. **Effects of Metrnβ on cardiomyocytes: protection against PE-induced hypertrophy in an autocrine manner. (a and b)** Cardiomyocyte size (a; CSA; data are representative of three independent experiments; P values are 0.0007, 0.0039, 0.0097, 0.0143, 0.0307, 0.0437) and mRNA expression levels (b) of the hypertrophy markers *Nppa* and *Acta1* in NCMs after PE-induced hypertrophy alone or with Metrnβ pretreatment for 24 h at different concentrations (data are representative of three independent experiments; P values are <0.0001, <0.0001, 0.0051, 0.0153, <0.0001, <0.0001). **(c and d)** Cardiomyocyte size (c; CSA; data are representative of three independent experiments; P values are 0.016, 0.0169) and mRNA expression levels [d] of the hypertrophy markers *Nppa* and *Acta1* in NCMs overexpressing Metrnβ (Ad-Metrnβ; blue bars) or Ad-null control vector (Ad-null; gray bars) at 10 IFU/cell and treated with PE for 24 h (data are representative of three independent experiments; P values are 0.0037, 0.0108, 0.0421, 0.0327, 0.0082). **(e)** α-SMA (*Acta2*) expression levels in Metrnβ (0.5 μg/ml)-treated primary culture CFs at P1 and P3 (data are representative of three independent experiments; P values are 0.002, 0.0065). **(f and g)** Cardiomyocyte size (f; CSA; data are representative of two independent experiments; P values are both <0.0001) and mRNA expression levels (g) of the hypertrophy markers *Nppa* and *Acta1* in NCMs treated with anti-Metrnβ antibody or control anti-IgG antibody added to the culture medium in the presence or

absence of PE (data are representative of two independent experiments; P values are 0.0015, 0.0181, 0.0002, 0.011, 0.0182). **(h)** Phosphorylation levels determined by Milliplex (left) and Western blot (right) of CREB and p38 in NCMs treated with Metrnβ (0.5 µg/ml) for different durations (data are representative of three independent experiments; P values are 0.0336, 0.0066). **(i)** Ppargc1a (PGC1α) expression levels in NCMs treated with different concentrations of Metrnβ for 24 h (data are representative of three independent experiments; P = 0.0007). Results are expressed as mean ± SEM. Data were analyzed by Student's *t* test (*, P < 0.05 compared with control cells; #, P < 0.05 compared with PE-treated or corresponding controls).

the most severe hypertrophy involving the basal IVS, interstitial fibrosis, aortic dilation, and left ventricular dysfunction. This phenotype, which shows a pattern more characteristic of cardiac dysfunction than of non-asymmetrical hypertrophy, resembles that in patients with hypertrophic cardiomyopathy (Marian and Braunwald, 2017; Yousefzai et al., 2017), one of the leading causes of sudden death among young people (Maron and Maron, 2013). Although it has been shown that hypertrophic cardiomyopathy may be inherited (Katayama et al., 2018), it seems unlikely that the effects observed in our global KO model are early development related, since basal signs of cardiac hypertrophy do not develop spontaneously in young Metrnβ-null mice. However, we cannot completely rule out this possibility, because Metrnβ has been reported to have effects on neuronal growth and brain development during embryogenesis (Jørgensen et al., 2012). Moreover, the abnormal hypertrophic response observed in Metrnβ-null mice is highly consistent, since it develops both after drug-induced hypertrophy and during the natural development of hypertrophy associated with aging. Nevertheless, we recognize the limitations of using a global *Metrnβ⁻/⁻* mouse model in terms of attributing cardiac alterations to the heart-specific loss of Metrnβ. Moreover, because *Metrnβ⁻/⁻* mice fully develop despite the complete absence

of the cytokine, these global KO mice may be viewed as an extreme model of Metrnβ function that also is unable to fully distinguish between developmental/aging and physiological effects.

The evidence that Metrnβ is cardioprotective may be viewed at first glance as paradoxical, given that we found high Metrnβ levels associated with cardiac pathology in humans and in mouse models. These high Metrnβ levels may be a reactive process to heart damage, which do not achieve full protection. Similar observations have been made for other cardiokines, such as ANF and FGF21 (Planavila et al., 2017; Planavila et al., 2013), which would share with Metrnβ protective actions upon the heart and high levels in cardiac pathology. The positive relationship between high levels of Metrnβ and cardiovascular death in our analysis of the prognostic value of Metrnβ levels is consistent with this scenario.

Although Metrnβ shows remarkable expression in the heart, its expression in the pericardium, skin, colon, trachea, tongue, and other mucosal sites is known to be much higher, suggesting a role for Metrnβ in native immunity (Ushach et al., 2015). In fact, Metrnβ expression has also been linked to inflammatory diseases, such as psoriasis, psoriatic and rheumatoid arthritis, and possibly sepsis (Ushach et al., 2015; Bridgewood et al., 2019).
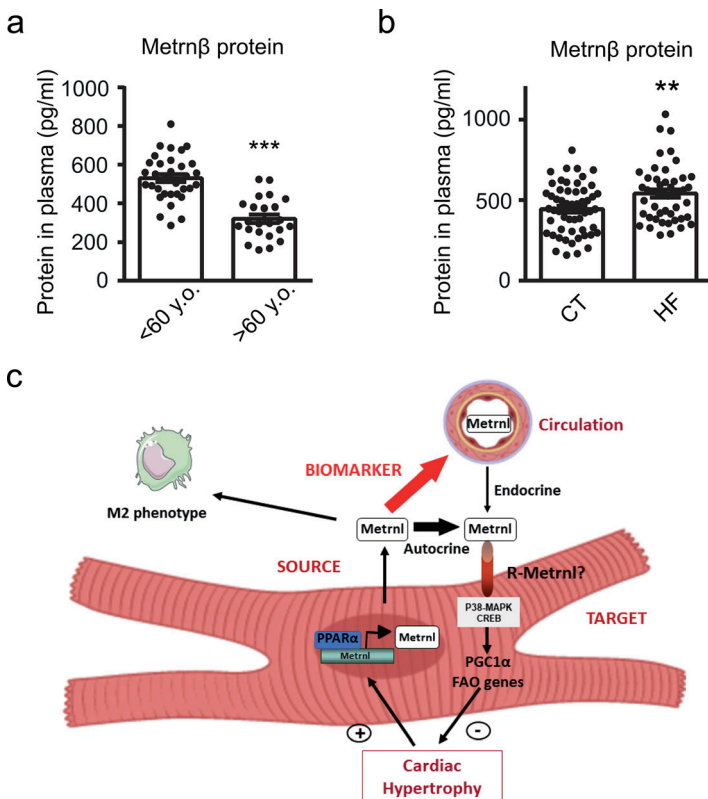

Figure 6. **Circulating levels of Metrnβ are regulated in humans. (a)** Plasma levels of Metrnβ in humans <60 yr old (mean age, 45 ± 1.35; *n* = 33) and >60 yr old (mean age, 80 ± 1.48; *n* = 23; P < 0.0001). **(b)** Plasma levels of Metrnβ in control (mean age, 60 ± 2.63; *n* = 56) and HF (mean age, 67 ± 1.7; *n* = 49) patients (P = 0.0093). Results are expressed as mean ± SEM. Data were analyzed by nonparametric Mann-Whitney test; **, P <0.001; ***, P < 0.0001 versus control patients. **(c)** Schematic representation of the transcriptional regulation and the endocrine and autocrine/paracrine actions of Metrnβ in the myocardium.

Table 4. Prognostic value of Metrnβ as a new biomarker for HF patients

	All-cause death			Cardiovascular death		
	HR	95% CI	P value	HR	95% CI	P value
Age, yr	1.06	1.04–1.07	<0.001	1.05	1.03–1.07	<0.001
Female	0.69	0.48–0.99	0.041	0.86	0.67–1.49	0.600
ZLog (Metrnl)	1.18	1.01–1.37	0.038	1.12	1.08–1.71	0.008
LVEF	1.01	1.00–1.02	0.191	1.00	0.99–1.02	0.720
Ischemia	1.07	0.79–1.46	0.646	1.70	1.10–2.65	0.018
Diabetes	1.33	0.99–1.80	0.062	1.26	0.82–1.93	0.300
Hypertension	1.06	0.75–1.48	0.758	1.03	0.62–1.71	0.920
Quartile						
Age, yr	1.05	1.04–1.07	<0.001	1.05	1.23–1.68	0.001
Female	0.69	0.48–0.99	0.043	1.00	0.97–1.02	0.650
ZLog (Metrnl)	1.26	1.09–1.45	0.002	1.46	1.23–1.68	0.001
LVEF	1.01	1.00–1.02	0.171	0.86	0.31–1.41	0.600
Ischemia	1.06	0.78–1.44	0.711	1.66	1.21–2.11	0.027
Diabetes	1.32	0–98–1.77	0.072	1.25	0.83–1.66	0.310
Hypertension	1.03	0.73–1.44	0.875	0.98	0.48–1.47	0.920

Multivariable analysis of cohort data of HF patients was performed following the Fine and Gray method from R essentials for SPSS. Values of Metrnβ were available for all patients and were log-transformed. ZLog, log-transformed and per 1 SD.

Consistent with this, *Metrnβ−/−* mice are more susceptible to septic shock and develop inflammatory lesions with aging (Ushach et al., 2018). An increase in the levels of Metrnβ in HF patients is consistent with this scenario, since inflammation is highly induced in HF patients. Moreover, Metrnβ levels are reduced in aging; thus, perhaps this low Metrnβ tone may confer an increased susceptibility to inflammation in the aged condition.

We found that the expression of Metrnβ in the heart is powerfully regulated by PPARα, which is in agreement with the cardioprotective role of Metrnβ. PPARα is known to strongly protect against heart damage, such as by blunting cardiac hypertrophy (Planavila et al., 2011; Smeets et al., 2008a), and the induction of Metrnβ may be one mechanism by which PPARα exert its protective actions.

In addition to the protective role of systemic Metrnβ on the heart, our data indicate that the local secretion of Metrnβ in the context of cardiac damage may serve as an endogenous autoregulatory means of cardioprotective signaling either in vitro or in vivo. Thus, the ability of Metrnβ-targeting antibodies to suppress the action of Metrnβ in cardiac cell cultures indicates that Metrnβ can act in an autocrine manner to protect cardiac cells from hypertrophic insults. Furthermore, the anti-hypertrophic effect of cardiac Metrnβ overexpression, mainly expressed in cardiomyocytes, in *Metrnβ−/−* mice also supports an autocrine capacity for this cardiokine.

The identity of the cellular receptor(s) mediating Metrnβ action is currently unknown. In cardiomyocytes, we herein reveal for the first time that Metrnβ treatment leads to the intracellular induction of p38-MAPK and to the phosphorylation of the transcription factor CREB, in contrast with findings in macrophages showing preferential induction of STAT3 phosphorylation by Metrnβ (Baht et al., 2020; Rao et al., 2014). Our observation that Metrnβ induces PGC1α in the heart both in vivo and in vitro is consistent with the known role of p38-MAPK induction and CREB phosphorylation in other cell systems, such as brown adipocytes (Villarroya et al., 2018). Our findings are also consistent with the known role of PGC1α as a cardioprotective actor (Aubert et al., 2013; Leone et al., 2005; Huss and Kelly, 2004) and with reports indicating that inactivation of p38-MAPK elicits cardiac hypertrophy in vivo (Braz et al., 2003). However, there is controversy regarding the general roles of p38-MAPK (Braz et al., 2003; Clerk et al., 1998) and CREB (Chien et al., 2015; Watson et al., 2007) activation in cardiac hypertrophy, and some reports have indicated that activation of p38-MAPK may promote cardiac hypertrophy (Streicher et al., 2010).

It is worth mentioning that although we found that Metrnβ has direct actions on cardiomyocytes, its protective effects in heart experimental models in vivo appear to involve a complex pattern of modifications, including the promotion of a noninflammatory environment in the myocardium. The involvement of Metrnβ in promoting anti-inflammatory effects is consistent with previous reports demonstrating that Metrnβ triggers increased M2 macrophage polarization in adipose tissues (Rao et al., 2014) and increases recruitment of immune cells to injured skeletal muscle (Baht et al., 2020). We also observed that Metrnβ reduced cardiac fibrosis in vivo but did not find that Metrnβ had any direct effect on CFs. Further research is needed to establish a comprehensive profile of the paracrine actions of cardiomyocyte-originating Metrnβ on the distinct cell types present in the heart, in addition to the autocrine effects on cardiomyocytes identified here. Moreover, further research will

also be needed to fully establish how much heart-derived Metrnβ contributes to the systemic levels of this protein, since some effects could also come from muscle secretion as well. This would allow us to identify a potential endocrine role of Metrnβ as a cardiokine and determine a biological rationale for assessing circulating Metrnβ levels in relation to cardiac pathology in patients.

Our identification of Metrnβ as a novel cardiokine has relevant biomedical implications. From a therapeutic viewpoint, our data indicate that long-term cardiac Metrnβ overexpression driven by the AAV9 subtype, with high cardiac tropism, could deserve future research as a potential gene therapy strategy against cardiac disease. However, although preferential expression in the heart, some AAV9-driven expression at other tissues, as shown here for muscle or in neural tissue according to Foust et al. (2009), may be a limitation. In any case, AAV-mediated gene therapy has an excellent record of efficacy and safety in vivo; in 2012, the European Union approved the first AAV-mediated in vivo gene therapy product, Glybera (alipogene tiparvovec), and others are currently in the pipeline (Büning, 2013). Moreover, based on data obtained from a large human cohort, we provide the first report indicating that Metrnβ has strong potential as a biomarker of heart disease.

In summary, our study indicates that Metrnβ shows promise as a new potential therapeutic agent for cardiac diseases and also as a new biomarker for prognosis in HF patients.

Materials and methods

Animals
Metrnβ-null mice (C57BL/6NTac-Metrnβ[tm1a(KOMP)Wtsi]/WtsiH; EM:07966) were obtained from the Wellcome Trust Sanger Institute Mouse Genetics Project. *Pparα*-null mice (B6.129S4-Pparα[tm1Gonz]/J) were obtained from The Jackson Laboratory. WT littermates were used as controls for all experiments with *Metrnβ*-null mice and *Pparα*-null mice. All experiments were performed in accordance with European Community Council Directive 86/609/EEC and were approved by the institutional animal care and use committee of the University of Barcelona.

Interventions in mice and echocardiography
To induce cardiac hypertrophy, 2-mo-old male age-matched WT and *Metrnβ*-null mice were anesthetized with 1.5% isoflurane, and Alzet osmotic minipumps containing PBS or ISO (the latter calibrated to release the drug at a rate of 15 mg/kg/d for 7 d) were surgically implanted subcutaneously in the interscapular region of each mouse.

To induce cardiac hypertrophy in neonates, 6-d-old WT and *PPARα*-null mice were subjected to i.p. injection of ISO (15 mg/kg/ d; Sigma) for 7 d, as previously reported (Planavila et al., 2011).

To induce hypertension, 2-mo-old WT mice were anesthetized with 1.5% isoflurane, and Alzet osmotic minipumps containing PBS or AngII; Sigma), the latter calibrated to release AngII at a rate of 1 mg/kg/d for 7 d, were surgically implanted subcutaneously in the interscapular region of each mouse (Ferrer-Curriu et al., 2019).

To perform TAC to induce cardiac hypertrophy, the chest of each mouse was opened, and the transverse aorta was ligated between the truncus brachiocephalicus and the left common carotid artery by tying a 6-0 silk suture against a 25-gauge needle. Mice were sacrificed 28 d after TAC or sham operation.

In all cases, analgesia was administered for 2 d after surgery (paracetamol 200 mg/kg/d).

In all cases, hypertrophy was assessed by echocardiography with a Vivid Q instrument (GE Healthcare) equipped with a 12-MHz microprobe. Ventricular measurements in M-mode and Doppler were made after 7 d of ISO treatment. Three different cardiac cycles were measured for each assessment, and average values were obtained. Analyses of echocardiographic images were performed by two different observers in a blinded manner.

AAV vectors
AAV9-null, AAV9-GFP, and AAV9-Metrnβ were generated by the Center for Animal Biotechnology and Gene Therapy (Barcelona, Spain) using a dual-triple plasmid cotransfection procedure followed by polyethylene glycol precipitation and purification through CsCl$_2$ gradient centrifugations. Mice were i.p. injected at 7 d of age with AAV9-null, AAV9-GFP, and AAV9-Metrnβ at a dose of 10^{13} viral genome particles per animal, as previously described (Raso et al., 2019).

Blood pressure and heart rate
Mouse blood pressure was measured using the tail-cuff method (BP2000; Visitech Systems). Mice were trained according to the manufacturer's instructions for 5 d before minipump implantation. 10 consecutive measurements were averaged to calculate the systolic, diastolic, and mean arterial blood pressures and heart rate during the 7-d period of minipump use.

Cell culture
Rat NCMs were obtained as previously described (Planavila et al., 2011). Briefly, hearts were digested with a collagenase solution (Collagenase Type I; Life Technologies, Ltd.) followed by differential plating. NCMs were stimulated with the α$_1$-adrenergic agonist PE (10 μmol/liter; Sigma), which is a hypertrophic growth factor, and/or the proinflammatory agents LPS (50 ng/ml; Sigma) or TNFα (50 ng/ml; Sigma). After treatment for 24–48 h, cells were harvested for RNA isolation. Where indicated, cells were treated with the PPARα antagonist GW6471 (1 μmol/liter; Sigma) or Metrnβ (OriGene Technologies, Inc.) for 24 h before being exposed to PE for an additional 24 h. Antibodies against IgG (Sigma) or Metrnβ (Santa Cruz Biotechnology, Inc.) were diluted 1:1,000 and added after the 24-h pretreatment period.

Rat neonatal CFs were isolated from the ventricles of 1–2-d-old Sprague-Dawley rats as described by Ferrer-Curriu et al. (2019). P1 and P3 cells were plated at a density of 0.3×10^5 cells/ cm^2 on culture dishes and grown for 24 h. Thereafter, the cells were serum starved for 24 h and then incubated with Metrnβ (50 nM) for another 24 h.

Adenoviral-mediated gene transduction
Recombinant adenoviruses expressing the murine Metrnβ cDNA and the murine PPARα cDNA were constructed as previously described (Ad5-CMV-Metrnβ and Ad5-CMV-PPARα,

respectively; Center for Animal Biotechnology and Gene Therapy; Amat et al., 2009). NCMs were infected with Metrnβ or PPARα Ads and the AdCMV-null control vector at 10 infectious units (IFUs)/cell for 24 h in serum-free medium.

Heart histology and immunohistochemistry in mice
Each heart was extracted and cut transversely at midheight. One half was fixed in 4% formaldehyde, embedded in paraffin, and sectioned. The sections were deparaffinized and stained with H&E for determination of cardiomyocyte size using ImageJ software. Fibrosis was determined by Masson's trichrome staining (Panreac). Formaldehyde-fixed, paraffin-embedded heart sections were incubated with a primary antibody against F4/80 (Abcam). Alexa Fluor 488–conjugated goat anti-rat IgG was used as the secondary antibody. Fluorescent micrographs were acquired under a fluorescent microscope (Olympus BX61).

RNA isolation and real-time RT-PCR
Total RNA was extracted using Tripure (Roche). RT was performed using a high-capacity RNA-to-cDNA kit (Applied Biosystems) and 0.5 µg RNA in a total reaction volume of 20 µl. PCR was conducted in duplicate for increased accuracy. TaqMan gene expression assays (Thermo Fisher Scientific) were used; each 25-µl reaction mixture contained 1 µl cDNA, 12.5 µl TaqMan Universal PCR Master Mix (Thermo Fisher Scientific), 250 nM probes, and 900 nM primers from the Assays-on-Demand Gene Expression Assay Mix or the Assays-by-Design Gene Expression Assay Mix (Thermo Fisher Scientific). Each sample was run in duplicate, and the mean value was used to calculate the mRNA expression of the gene of interest and the housekeeping reference gene (cyclophilin A, PPIA). The mRNA level of the gene of interest in each sample was normalized to that of the reference control using the comparative $2^{-\Delta CT}$ method.

Analysis of plasma metabolites and protein phosphorylation
Glucose and triglyceride levels were measured using the Accutrend Technology system (Roche Diagnostics). Metrnβ protein levels in plasma and in NCM culture media were detected using an Metrnβ ELISA kit (R&D Systems). Protein phosphorylation in NCMs was assessed using the Milliplex MAP 9-plex Multi-Pathway Signaling Magnetic Bead kit (Merck-Millipore) for phosphorylated and total proteins.

Western blotting
Western blot analyses were performed using antibodies against α-SMA (Sigma), PGC1α (Santa Cruz Biotechnology), phospho-p38, p38, phospho-CREB, CREB (all from Cell Signaling Technology), and GAPDH (Sigma). Whole-cell lysates were obtained as previously described (Planavila et al., 2005a), and proteins were separated by 10% SDS-PAGE and transferred to Immobilon-P membranes (Millipore).

Cardiac human biopsies for gene expression analysis
Human hearts were obtained from patients with dilated cardiomyopathy and final-stage HF who underwent cardiac transplant (five patients). Controls were obtained from heart samples from organ donors without a clinical history of HF and whose heart could not be used for any reason (six controls; Planavila et al., 2015). Written informed consent was obtained from all participants in the human population study, which conformed to the principles outlined in the Declaration of Helsinki. The study was approved by the institutional ethical committee of the Hospital Clinic of Barcelona (Barcelona, Spain) following standard procedures.

Cardiac human biopsies for histology
Hearts from donors under 70 yr of age with brain death of cerebrovascular or traumatic origin were routinely evaluated for possible transplantation at the transplant unit of the Hospital Clinic (Ferrer-Curriu et al., 2019). From these samples, 6 control hearts were collected from healthy normotensive individuals (controls), and 21 hearts were obtained from donors with long-standing hypertension (cases) who were not eligible for transplantation because of lack of a matched recipient or inadequate size. Of these 21 hearts, 10 exhibited clinical and echosonographical criteria for dilated cardiomyopathy. We also collected three hearts with idiopathic cardiomyopathy and five hearts with valvular cardiomyopathy. The study protocol was approved by the ethics committee of the Hospital Clinic (Barcelona, Spain; reference HCB/2015/0233), and informed consent regarding the use of myocardial tissue for this research was obtained from the families of donors before the study. The authors of this article certify compliance with the statement on ethics outlined in the Declaration of Helsinki of 1975, as revised in 1983.

Human histological studies
Myocardial expression of Metrnβ was measured by immunostaining with an anti-Metrnβ antibody (Abcam). 6 areas of each sample were evaluated, and a total of 200–600 cells were assessed per field (≥1,200 cells/sample). The Metrnβ expression index was calculated as the ratio of positively stained to negatively stained myocytes. Immunohistochemical evaluations were performed by two independent evaluators.

Human plasma samples
From May 2009 to April 2014, ambulatory patients treated at a multidisciplinary HF clinic were consecutively included in the study. The referral inclusion criteria and blood sample collection were described elsewhere (Lupón et al., 2013; Bayés-Genís et al., 2015; Bayes-Genis et al., 2012). All analyses of biomarkers were performed on the same blood sample, which had been stored at –80°C without any prior freeze–thaw cycle. All samples were obtained between 9:00 a.m. and 12:00 p.m. All participants provided written informed consent, and the ethics committee of Hospital Germans Trias i Pujol (Badalona, Spain) approved the study. All study procedures were performed in accordance with the ethical standards outlined in the Helsinki Declaration of 1975, revised in 1983.

The primary endpoint was all-cause death. Cardiovascular death was also assessed. A death was considered to be cardiovascular in origin when it was caused by HF (decompensated HF or treatment-resistant HF, in the absence of another cause), sudden death (unexpected death, witnessed or not, of a previously stable patient with no evidence of worsening HF or any

Rupérez et al.
Meteorin-β protects the myocardium

Journal of Experimental Medicine   16 of 18
https://doi.org/10.1084/jem.20201206

other cause of death), acute myocardial infarction (due to mechanical, hemodynamic, or arrhythmic complications), stroke (in association with recent acute neurological deficits), a procedural death (after diagnostic or therapeutic cardiovascular procedures), and other cardiovascular causes (e.g., rupture of an aneurysm, peripheral ischemia, or aortic dissection). For discriminant analyses, Harrell's C-statistic, which takes into account time to the event, unlike the usually used area under the curve, was obtained. Computations were done following the Fine and Gray method from R essentials for SPSS, using the R package cmprsk, which was built by Bob Gray using R version 3.2.5.

Statistics

Cell culture experiments were conducted on at least two independent cardiomyocyte isolations. We used five or six mice/group in the in vivo experiments. Results are presented as mean ± SEM. Data were analyzed by t test, one- and two-way ANOVA, or Mann-Whitney test, followed by post hoc tests as appropriate, using GraphPad Prism software (GraphPad Software Inc.). A P value <0.05 was considered statistically significant.

Online supplemental material

Fig. S1 shows the results of Metrnβ expression levels in human samples and the experiments to assess AAV9 infection in mice. Fig. S2 shows the results of antiapoptotic genes in mice and the effects of proinflammatory stimuli in cardiomyocytes. Table S1 shows morphometric and metabolic profiles of mice. Table S2 shows blood pressure results in mice. Table S3 shows baseline demographic and clinical characteristics of the HF patient cohort.

References

Amat, R., A. Planavila, S.L. Chen, R. Iglesias, M. Giralt, and F. Villarroya. 2009. SIRT1 controls the transcription of the peroxisome proliferator-activated receptor-gamma co-activator-1alpha (PGC-1alpha) gene in skeletal muscle through the PGC-1alpha autoregulatory loop and interaction with MyoD. *J. Biol. Chem.* 284:21872–21880. https://doi.org/10.1074/jbc.M109.022749

Aubert, G., R.B. Vega, and D.P. Kelly. 2013. Perturbations in the gene regulatory pathways controlling mitochondrial energy production in the failing heart. *Biochim. Biophys. Acta.* 1833:840–847. https://doi.org/10.1016/j.bbamcr.2012.08.015

Baht, G.S., A. Bareja, D.E. Lee, R.R. Rao, R. Huang, J.L. Huebner, D.B. Bartlett, C.R. Hart, J.R. Gibson, I.R. Lanza, et al. 2020. Meteorin-like facilitates skeletal muscle repair through a Stat3/IGF-1 mechanism. *Nat. Metab.* 2:278–289. https://doi.org/10.1038/s42255-020-0184-y

Bär, C., B. Bernardes de Jesus, R. Serrano, A. Tejera, E. Ayuso, V. Jimenez, I. Formentini, M. Bobadilla, J. Mizrahi, A. de Martino, et al. 2014. Telomerase expression confers cardioprotection in the adult mouse heart after acute myocardial infarction. *Nat. Commun.* 5:5863. https://doi.org/10.1038/ncomms6863

Bayes-Genis, A., M. de Antonio, A. Galán, H. Sanz, A. Urrutia, R. Cabanes, L. Cano, B. González, C. Díez, T. Pascual, et al. 2012. Combined use of high-sensitivity ST2 and NTproBNP to improve the prediction of death in heart failure. *Eur. J. Heart Fail.* 14:32–38. https://doi.org/10.1093/eurjhf/hfr156

Bayés-Genís, A., J. Barallat, A. Galán, M. de Antonio, M. Domingo, E. Zamora, A. Urrutia, and J. Lupón. 2015. Soluble neprilysin is predictive of cardiovascular death and heart failure hospitalization in heart failure patients. *J. Am. Coll. Cardiol.* 65:657–665. https://doi.org/10.1016/j.jacc.2014.11.048

Braz, J.C., O.F. Bueno, Q. Liang, B.J. Wilkins, Y.S. Dai, S. Parsons, J. Braunwart, B.J. Glascock, R. Klevitsky, T.F. Kimball, et al. 2003. Targeted inhibition of p38 MAPK promotes hypertrophic cardiomyopathy through upregulation of calcineurin-NFAT signaling. *J. Clin. Invest.* 111:1475–1486. https://doi.org/10.1172/JCI200317295

Bridgewood, C., T. Russell, H. Weedon, T. Baboolal, A. Watad, K. Sharif, R. Cuthbert, M. Wittmann, M. Wechalekar, and D. McGonagle. 2019. The novel cytokine Metrnl/IL-41 is elevated in psoriatic arthritis synovium and inducible from both entheseal and synovial fibroblasts. *Clin. Immunol.* 208:108253. https://doi.org/10.1016/j.clim.2019.108253

Büning, H. 2013. Gene therapy enters the pharma market: the short story of a long journey. *EMBO Mol. Med.* 5:1–3. https://doi.org/10.1002/emmm.201202291

Cereijo, R., A. Gavaldà-Navarro, M. Cairó, T. Quesada-López, J. Villarroya, S. Morón-Ros, D. Sánchez-Infantes, M. Peyrou, R. Iglesias, T. Mampel, et al. 2018. CXCL14, a brown adipokine that mediates brown-fat-to-macrophage communication in thermogenic adaptation. *Cell Metab.* 28:750–763.e6. https://doi.org/10.1016/j.cmet.2018.07.015

Chien, P.T., C.C. Lin, L.D. Hsiao, and C.M. Yang. 2015. c-Src/Pyk2/EGFR/PI3K/Akt/CREB-activated pathway contributes to human cardiomyocyte hypertrophy: role of COX-2 induction. *Mol. Cell. Endocrinol.* 409:59–72. https://doi.org/10.1016/j.mce.2015.04.005

Clerk, A., A. Michael, and P.H. Sugden. 1998. Stimulation of the p38 mitogen-activated protein kinase pathway in neonatal rat ventricular myocytes by the G protein-coupled receptor agonists, endothelin-1 and phenylephrine: a role in cardiac myocyte hypertrophy? *J. Cell Biol.* 142:523–535. https://doi.org/10.1083/jcb.142.2.523

Doroudgar, S., and C.C. Glembotski. 2011. The cardiokine story unfolds: ischemic stress-induced protein secretion in the heart. *Trends Mol. Med.* 17:207–214. https://doi.org/10.1016/j.molmed.2010.12.003

Ferrer-Curriu, G., I. Redondo-Angulo, M. Guitart-Mampel, C. Ruperez, A. Mas-Stachurska, M. Sitges, G. Garrabou, F. Villarroya, J. Fernández-Solà, and A. Planavila. 2019. Fibroblast growth factor-21 protects against fibrosis in hypertensive heart disease. *J. Pathol.* 248:30–40. https://doi.org/10.1002/path.5226

Foust, K.D., E. Nurre, C.L. Montgomery, A. Hernandez, C.M. Chan, and B.K. Kaspar. 2009. Intravascular AAV9 preferentially targets neonatal neurons and adult astrocytes. *Nat. Biotechnol.* 27:59–65. https://doi.org/10.1038/nbt.1515

Hu, C., X. Zhang, P. Song, Y.P. Yuan, C.Y. Kong, H.M. Wu, S.C. Xu, Z.G. Ma, and Q.Z. Tang. 2020. Meteorin-like protein attenuates doxorubicin-induced cardiotoxicity via activating cAMP/PKA/SIRT1 pathway. *Redox Biol.* 37:101747. https://doi.org/10.1016/j.redox.2020.101747

Huss, J.M., and D.P. Kelly. 2004. Nuclear receptor signaling and cardiac energetics. *Circ. Res.* 95:568–578. https://doi.org/10.1161/01.RES.0000141774.29937.e3

Jørgensen, J.R., A. Fransson, L. Fjord-Larsen, L.H. Thompson, J.P. Houchins, N. Andrade, M. Torp, N. Kalkkinen, E. Andersson, O. Lindvall, et al. 2012. Cometin is a novel neurotrophic factor that promotes neurite outgrowth and neuroblast migration in vitro and supports survival of spiral ganglion neurons in vivo. *Exp. Neurol.* 233:172–181. https://doi.org/10.1016/j.expneurol.2011.09.027

Jung, T.W., S.H. Lee, H.C. Kim, J.S. Bang, A.M. Abd El-Aty, A. Hacımüftüoğlu, Y.K. Shin, and J.H. Jeong. 2018. METRNL attenuates lipid-induced inflammation and insulin resistance via AMPK or PPARδ-dependent pathways in skeletal muscle of mice. *Exp. Mol. Med.* 50:122. https://doi.org/10.1038/s12276-018-0147-5

Katayama, M., P.M. Panse, C.B. Kendall, J.R. Daniels, S.S. Cha, F.D. Fortuin, J.P. Sweeney, P.A. DeValeria, L.A. Lanza, M. Belohlavek, et al. 2018. Left ventricular septal hypertrophy in elderly patients with aortic stenosis. *J. Ultrasound Med.* 37:217–224. https://doi.org/10.1002/jum.14320

Lee, J.H., Y.E. Kang, J.M. Kim, S. Choung, K.H. Joung, H.J. Kim, and B.J. Ku. 2018. Serum Meteorin-like protein levels decreased in patients newly diagnosed with type 2 diabetes. *Diabetes Res. Clin. Pract.* 135:7–10. https://doi.org/10.1016/j.diabres.2017.10.005

Leone, T.C., J.J. Lehman, B.N. Finck, P.J. Schaeffer, A.R. Wende, S. Boudina, M. Courtois, D.F. Wozniak, N. Sambandam, C. Bernal-Mizrachi, et al. 2005. PGC-1α deficiency causes multi-system energy metabolic derangements: muscle dysfunction, abnormal weight control and hepatic steatosis. *PLoS Biol.* 3:e101. https://doi.org/10.1371/journal.pbio.0030101

Li, Z.Y., J. Song, S.L. Zheng, M.B. Fan, Y.F. Guan, Y. Qu, J. Xu, P. Wang, and C.Y. Miao. 2015. Adipocyte Metrnl antagonizes insulin resistance through PPARγ signaling. *Diabetes.* 64:4011–4022. https://doi.org/10.2337/db15-0274

Liu, Z.X., H.H. Ji, M.P. Yao, L. Wang, Y. Wang, P. Zhou, Y. Liu, X.F. Zheng, H.W. He, L.S. Wang, et al. 2019. Serum Metrnl is associated with the presence and severity of coronary artery disease. *J. Cell. Mol. Med.* 23:271–280. https://doi.org/10.1111/jcmm.13915

Lupón, J., M. de Antonio, A. Galán, J. Vila, E. Zamora, A. Urrutia, and A. Bayes-Genis. 2013. Combined use of the novel biomarkers high-sensitivity troponin T and ST2 for heart failure risk stratification vs conventional assessment. *Mayo Clin. Proc.* 88:234–243. https://doi.org/10.1016/j.mayocp.2012.09.016

Marian, A.J., and E. Braunwald. 2017. Hypertrophic cardiomyopathy: genetics, pathogenesis, clinical manifestations, diagnosis, and therapy. *Circ. Res.* 121:749–770. https://doi.org/10.1161/CIRCRESAHA.117.311059

Maron, B.J., and M.S. Maron. 2013. Hypertrophic cardiomyopathy. *Lancet.* 381:242–255. https://doi.org/10.1016/S0140-6736(12)60397-3

Pellitero, S., I. Piquer-Garcia, G. Ferrer-Curriu, R. Puig, E. Martínez, P. Moreno, J. Tarascó, J. Balibrea, C. Lerin, M. Puig-Domingo, et al. 2018. Opposite changes in Meteorin-like and oncostatin M levels are associated with metabolic improvements after bariatric surgery. *Int. J. Obes.* 42:919–922. https://doi.org/10.1038/ijo.2017.268

Planavila, A., J.C. Laguna, and M. Vázquez-Carrera. 2005a. Atorvastatin improves peroxisome proliferator-activated receptor signaling in cardiac hypertrophy by preventing nuclear factor-kappa B activation. *Biochim. Biophys. Acta.* 1687:76–83. https://doi.org/10.1016/j.bbalip.2004.11.004

Planavila, A., J.C. Laguna, and M. Vázquez-Carrera. 2005b. Nuclear factor-kappaB activation leads to down-regulation of fatty acid oxidation during cardiac hypertrophy. *J. Biol. Chem.* 280:17464–17471. https://doi.org/10.1074/jbc.M414220200

Planavila, A., R. Iglesias, M. Giralt, and F. Villarroya. 2011. Sirt1 acts in association with PPARα to protect the heart from hypertrophy, metabolic

dysregulation, and inflammation. *Cardiovasc. Res.* 90:276–284. https://doi.org/10.1093/cvr/cvq376

Planavila, A., I. Redondo, E. Hondares, M. Vinciguerra, C. Munts, R. Iglesias, L.A. Gabrielli, M. Sitges, M. Giralt, M. van Bilsen, et al. 2013. Fibroblast growth factor 21 protects against cardiac hypertrophy in mice. *Nat. Commun.* 4:2019. https://doi.org/10.1038/ncomms3019

Planavila, A., I. Redondo-Angulo, F. Ribas, G. Garrabou, J. Casademont, M. Giralt, and F. Villarroya. 2015. Fibroblast growth factor 21 protects the heart from oxidative stress. *Cardiovasc. Res.* 106:19–31. https://doi.org/10.1093/cvr/cvu263

Planavila, A., J. Fernández-Solà, and F. Villarroya. 2017. Cardiokines as modulators of stress-induced cardiac disorders. *Adv. Protein Chem. Struct. Biol.* 108:227–256. https://doi.org/10.1016/bs.apcsb.2017.01.002

Rao, R.R., J.Z. Long, J.P. White, K.J. Svensson, J. Lou, I. Lokurkar, M.P. Jedrychowski, J.L. Ruas, C.D. Wrann, J.C. Lo, et al. 2014. Meteorin-like is a hormone that regulates immune-adipose interactions to increase beige fat thermogenesis. *Cell.* 157:1279–1291. https://doi.org/10.1016/j.cell.2014.03.065

Raso, A., E. Dirkx, L.E. Philippen, A. Fernandez-Celis, F. De Majo, V. Sampaio-Pinto, M. Sansonetti, R. Juni, H. El Azzouzi, M. Calore, et al. 2019. Therapeutic delivery of miR-148a suppresses ventricular dilation in heart failure. *Mol. Ther.* 27:584–599. https://doi.org/10.1016/j.ymthe.2018.11.011

Redondo-Angulo, I., A. Mas-Stachurska, M. Sitges, M. Giralt, F. Villarroya, and A. Planavila. 2016. C/EBPβ is required in pregnancy-induced cardiac hypertrophy. *Int. J. Cardiol.* 202:819–828. https://doi.org/10.1016/j.ijcard.2015.10.005

Smeets, P.J., A. Planavila, G.J. van der Vusse, and M. van Bilsen. 2007. Peroxisome proliferator-activated receptors and inflammation: take it to heart. *Acta Physiol. (Oxf.).* 191:171–188. https://doi.org/10.1111/j.1748-1716.2007.01752.x

Smeets, P.J., B.E. Teunissen, A. Planavila, H. de Vogel-van den Bosch, P.H. Willemsen, G.J. van der Vusse, and M. van Bilsen. 2008a. Inflammatory pathways are activated during cardiomyocyte hypertrophy and attenuated by peroxisome proliferator-activated receptors PPARalpha and PPARdelta. *J. Biol. Chem.* 283:29109–29118. https://doi.org/10.1074/jbc.M802143200

Smeets, P.J., B.E. Teunissen, P.H. Willemsen, F.A. van Nieuwenhoven, A.E. Brouns, B.J. Janssen, J.P. Cleutjens, B. Staels, G.J. van der Vusse, and M. van Bilsen. 2008b. Cardiac hypertrophy is enhanced in PPARα$^{-/-}$ mice in response to chronic pressure overload. *Cardiovasc. Res.* 78:79–89. https://doi.org/10.1093/cvr/cvn001

Streicher, J.M., S. Ren, H. Herschman, and Y. Wang. 2010. MAPK-activated protein kinase-2 in cardiac hypertrophy and cyclooxygenase-2 regulation in heart. *Circ. Res.* 106:1434–1443. https://doi.org/10.1161/CIRCRESAHA.109.213199

Teunissen, B.E., P.J. Smeets, P.H. Willemsen, L.J. De Windt, G.J. Van der Vusse, and M. Van Bilsen. 2007. Activation of PPARdelta inhibits cardiac fibroblast proliferation and the transdifferentiation into myofibroblasts. *Cardiovasc. Res.* 75:519–529. https://doi.org/10.1016/j.cardiores.2007.04.026

Ushach, I., A.M. Burkhardt, C. Martinez, P.A. Hevezi, P.A. Gerber, B.A. Buhren, H. Schrumpf, R. Valle-Rios, M.I. Vazquez, B. Homey, et al. 2015. Meteorin-like is a cytokine associated with barrier tissues and alternatively activated macrophages. *Clin. Immunol.* 156:119–127. https://doi.org/10.1016/j.clim.2014.11.006

Ushach, I., G. Arrevillaga-Boni, G.N. Heller, E. Pone, M. Hernandez-Ruiz, J. Catalan-Dibene, P. Hevezi, and A. Zlotnik. 2018. Meteorin-like/Meteorin-β is a novel immunoregulatory cytokine associated with inflammation. *J. Immunol.* 201:3669–3676. https://doi.org/10.4049/jimmunol.1800435

van Bilsen, M., G.J. van der Vusse, and R.S. Reneman. 1998. Transcriptional regulation of metabolic processes: implications for cardiac metabolism. *Pflugers Arch.* 437:2–14. https://doi.org/10.1007/s004240050739

Villarroya, F., R. Cereijo, J. Villarroya, A. Gavaldà-Navarro, and M. Giralt. 2018. Toward an understanding of how immune cells control brown and beige adipobiology. *Cell Metab.* 27:954–961. https://doi.org/10.1016/j.cmet.2018.04.006

Watson, P.A., J.E. Reusch, S.A. McCune, L.A. Leinwand, S.W. Luckey, J.P. Konhilas, D.A. Brown, A.J. Chicco, G.C. Sparagna, C.S. Long, et al. 2007. Restoration of CREB function is linked to completion and stabilization of adaptive cardiac hypertrophy in response to exercise. *Am. J. Physiol. Heart Circ. Physiol.* 293:H246–H259. https://doi.org/10.1152/ajpheart.00734.2006

Yousefzai, R., A. Agarwal, M. Fuad Jan, C. Cho, M. Anigbogu, K. Shetabi, M. Singh, M. Bush, S. Treiber, S. Port, et al. 2017. Hypertrophic cardiomyopathy with aortic dilation: a novel observation. *Eur. Heart J. Cardiovasc. Imaging.* 18:1398–1403. https://doi.org/10.1093/ehjci/jew292
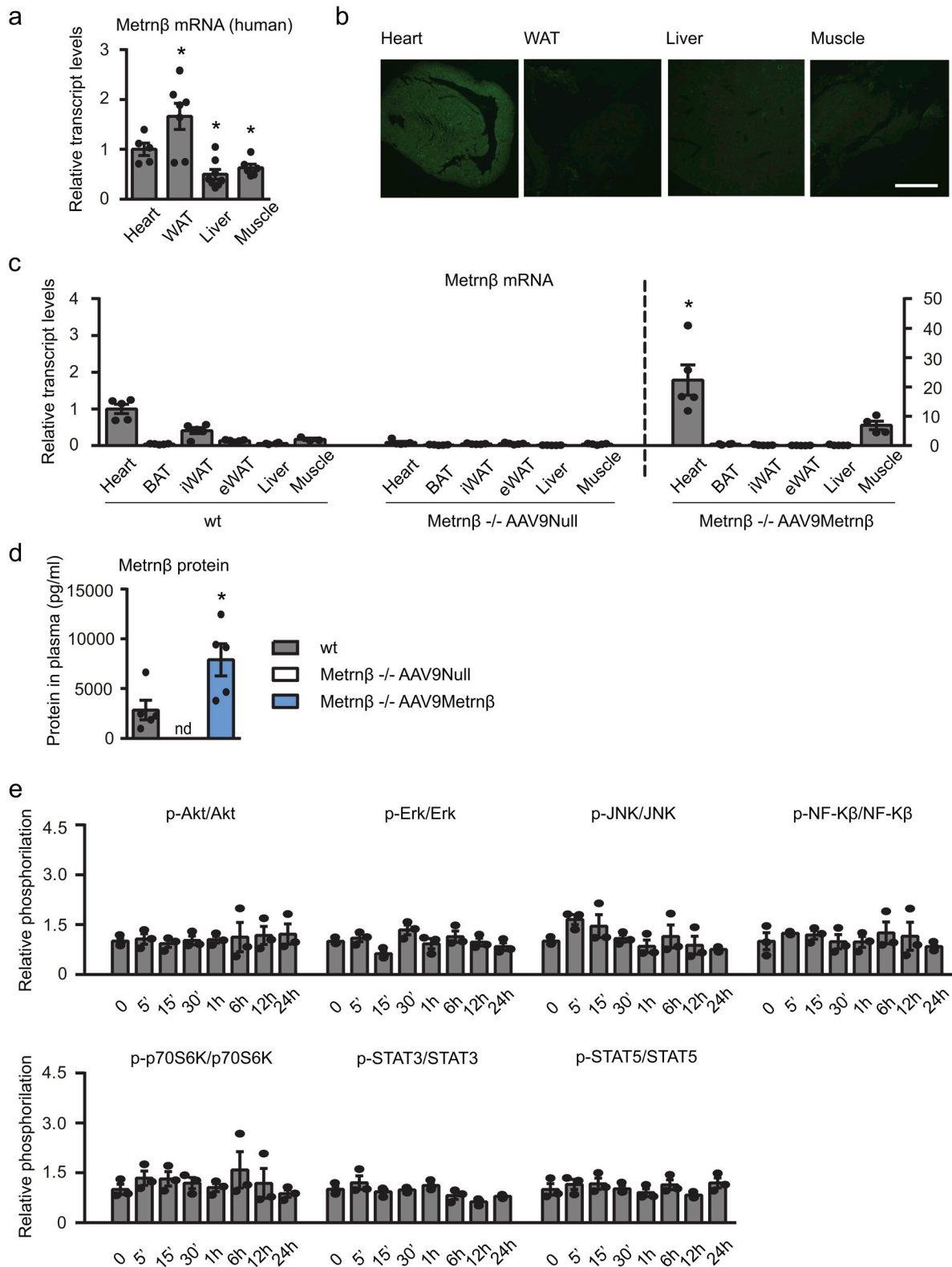
Supplemental material

Figure S1. **Metrnβ overexpression in the myocardium. (a)** Metrnβ mRNA expression levels in human samples from heart ($n = 5$), adipose tissue ($n = 7$), liver ($n = 8$), and skeletal muscle ($n = 7$; Student's t test; P values are 0.0226, 0.0096, 0.0261 versus heart). **(b)** Anti-GFP immunohistochemistry to assess tropism of AAV9-GFP viruses to the myocardium. Scale bar, 2 mm. **(c)** Expression levels of Metrnβ in several tissues of WT and *Metrnβ*^{−/−} mice injected with AAV9-Metrnβ or AAV9-null; $n = 5$ mice/group (Student's t test; P = 0.0033 versus WT mice). **(d)** Circulating Metrnβ levels of WT and *Metrnβ*^{−/−} mice injected with AAV9-Metrnβ (blue bars) or AAV9-null (white bars); $n = 5$ mice/group (Student's t test; P = 0.0283 versus WT mice). **(e)** Phosphorylation levels of different proteins in NCMs treated with Metrnβ (0.5 µg/ml) during different times. Cell culture experiments were conducted on three independent cardiomyocyte isolations. Results are expressed as mean ± SEM. *, P < 0.05 compared with heart (a) and with corresponding WT mice (c and d).
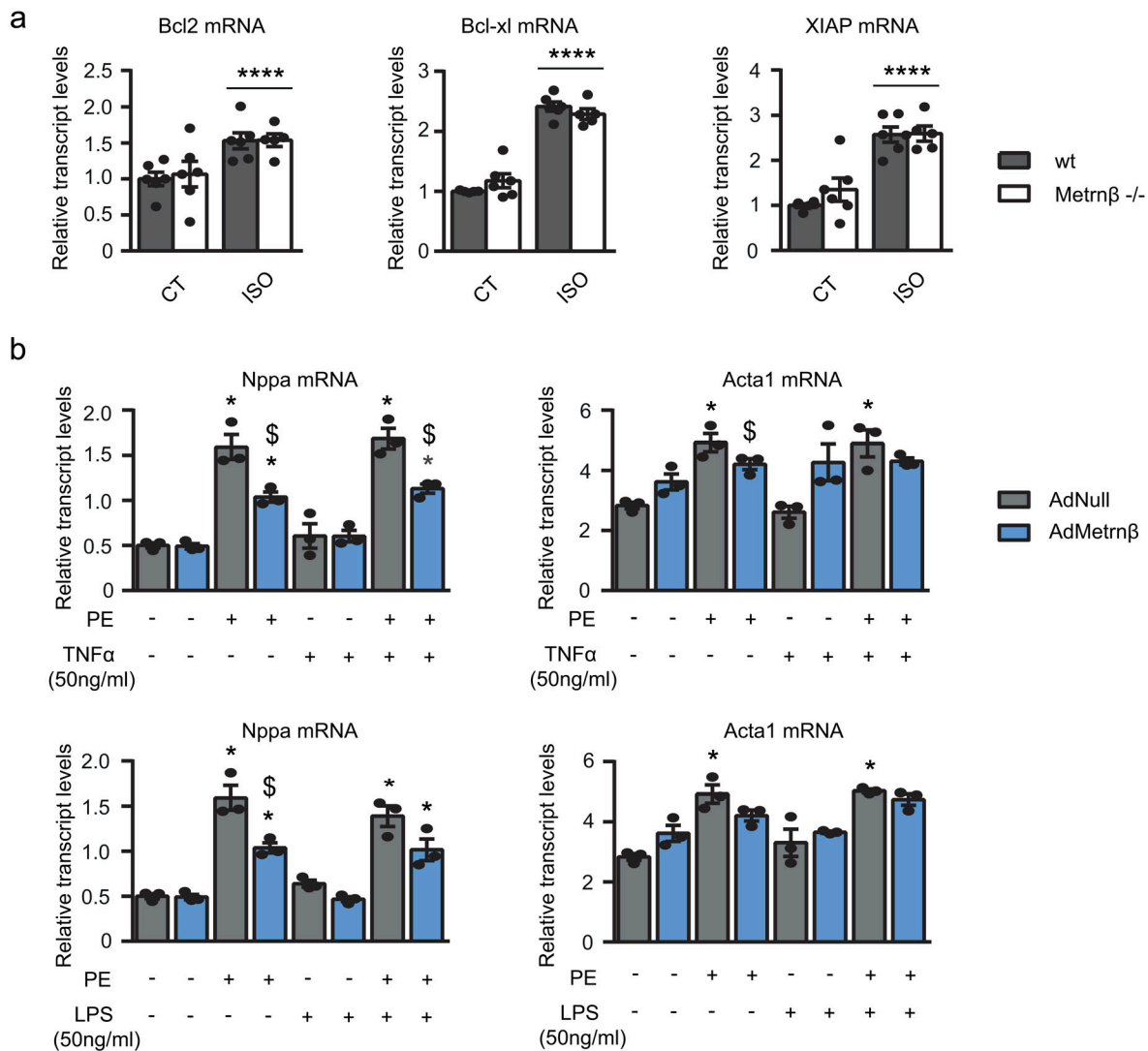
Figure S2. **Role of Metrnβ in apoptotic and pro-inflammatory pathways. (a)** 2-mo-old WT littermates (gray bars) and *Metrnβ⁻/⁻* (white bars) mice were continuously infused with ISO for 7 d to experimentally induce heart hypertrophy. mRNA expression levels of antiapoptotic genes *Bcl2, Bcl-xl, and Xiap* in the myocardium. *n* = 6 mice/group. Data were analyzed by two-way ANOVA (****, P < 0.00001 compared with corresponding control [CT] mice). **(b)** mRNA expression levels of the hypertrophy markers *Nppa* and *Acta1* in NCMs after PE-induced hypertrophy alone or with TNFα or LPS in NCMs overexpressing Metrnβ (Ad-Metrnβ; blue bars) or Ad-null control vector (10 IFU/cell; gray bars). Cell culture experiments were conducted on three independent cardiomyocyte isolations. Data were analyzed by Student's *t* test. Results are expressed as mean ± SEM (P values are 0.0015, 0.02, 0.001, 0.0036, 0.003, 0.011, 0.0028, 0.0492, 0.0096, 0.0015, 0.02, 0.001, 0.0035, 0.0114, 0.0028, 0.0196; *, P < 0.05 compared with control cells; $, P < 0.05 compared with PE-treated cells).

Three tables are available online. Table S1 displays the morphometric and metabolic profiles of WT and *Metrnβ⁻/⁻* mice. Table S2 provides the blood pressure in WT and *Metrnβ⁻/⁻* mice and *Metrnβ⁻/⁻* mice injected with AAV9-Metrnβ or AAV9-null. Table S3 lists the baseline demographic and clinical characteristics of a cohort of 446 patients with HF.